nature materials

Article

https://doi.org/10.1038/s41563-024-01909-w

Inulin-gel-based oral immunotherapy remodels the small intestinal microbiome and suppresses food allergy

Received: 4 December 2022

Accepted: 30 April 2024

Published online: 08 July 2024

Check for updates

Kai Han[1,2,13,14], Fang Xie[1,2,14], Olamide Animasahun[2,3,4], Minal Nenwani[2,3,4], Sho Kitamoto[5], Yeji Kim[5], May Thazin Phoo[1], Jin Xu[1,2], Fulei Wuchu[2,3,4], Kehinde Omoloja[2,3,4], Abhinav Achreja[2,3,4], Srinadh Choppara[2,3,4], Zhaoheng Li[6], Wang Gong[7], Young Seok Cho[1,2], Hannah Dobson[1,2], Jinsung Ahn[1,2,8], Xingwu Zhou[1,2], Xuehui Huang[1,2], Xinran An[1], Alexander Kim[1], Yao Xu[1,2], Qi Wu[1,2], Soo-Hong Lee[8], Jessica J. O'Konek[9], Yuying Xie[10,11], Yu Leo Lei[7], Nobuhiko Kamada[5,12], Deepak Nagrath[2,3,4] & James J. Moon[1,2,3,4]

Despite the potential of oral immunotherapy against food allergy, adverse reactions and loss of desensitization hinder its clinical uptake. Dysbiosis of the gut microbiota is implicated in the increasing prevalence of food allergy, which will need to be regulated to enable for an effective oral immunotherapy against food allergy. Here we report an inulin gel formulated with an allergen that normalizes the dysregulated ileal microbiota and metabolites in allergic mice, establishes allergen-specific oral tolerance and achieves robust oral immunotherapy efficacy with sustained unresponsiveness in food allergy models. These positive outcomes are associated with enhanced allergen uptake by antigen-sampling dendritic cells in the small intestine, suppressed pathogenic type 2 immune responses, increased interferon-γ$^+$ and interleukin-10$^+$ regulatory T cell populations, and restored ileal abundances of *Eggerthellaceae* and *Enterorhabdus* in allergic mice. Overall, our findings underscore the therapeutic potential of the engineered allergen gel as a suitable microbiome-modulating platform for food allergy and other allergic diseases.

Food allergy has become a major public health concern across the globe, particularly in industrialized countries. Accidental exposure to allergens can provoke life-threatening hypovolemic shock, and the interventions have long been limited to strict allergen avoidance, emergency treatments and experimental therapy[1]. The US Food and Drug Administration (FDA) recently approved the first oral immunotherapy (OIT) drug, Palforzia, which reduces the incidence and severity of allergic reactions to peanuts by dampening the pathological type 2 immune responses[2]. However, 10–20% of patients discontinue Palforzia owing to adverse events, with gastrointestinal events as the most common reason[3]. Moreover, most patients fail to develop long-lived sustained unresponsiveness due to dosing intermittence, insufficient daily maintenance dose during OIT or OIT cessation for just 2–24 weeks[4,5].

Growing evidence supports a link between gut dysbiosis, microbial metabolites and food allergy[6,7]. Bacteriotherapy, including faecal microbiota transplantation and probiotics, has been reported to restore the healthy intestinal microbiota and promote allergen desensitization, with microbial metabolites being revealed as a crucial link[8]. However, safety concerns, lack of consensus on a core set of favourable microbial species and poor engraftment rate largely

A full list of affiliations appears at the end of the paper. e-mail: moonjj@umich.edu

limit its clinical applications[9]. In particular, previous studies on how the gut microbiome promotes allergen desensitization have primarily focused on analysing faecal samples for the gut commensals and certain microbial metabolites, including short-chain fatty acids and bile acids[5,10]. Although faecal sampling is a non-invasive and convenient method, faecal samples are an approximation of the whole gut microbiome owing to regional differences along the gastrointestinal tract[11–13]. Importantly, antigenic priming and tolerance to food antigens begin in the small intestine[14], and emerging evidence suggests a crucial role of the microbiota and metabolites of the small intestine in food allergy[15]. Yet, it remains unknown how to modulate intestinal microorganisms and their metabolites for therapeutic intervention against food allergy.

Delivery of dietary antigens to antigen-sampling dendritic cells (DCs) of the small intestine is crucial for gut homoeostasis and oral tolerance[16]. However, the mean transit time in the small intestine is short (60–70 min in mice and humans[17,18]), thereby limiting the antigen-sampling process and tolerance induction during OIT[19]. We have previously reported an oral prebiotic-based gel that can prolong gastric emptying and gastrointestinal residence time[20]. Here we have engineered a novel OIT platform based on inulin gel for oral antigen delivery to intestinal DCs and in situ modulation of the microbiome–metabolites–immune axis. We demonstrate that inulin gel formulated with food allergen prolongs the intestinal retention of both inulin and allergen, and improves allergen uptake by tolerogenic DCs in the small intestine. Inulin-gel-based OIT suppressed T helper 2 (T_H2) cell subsets and induced IFNγ$^+$ and IL-10$^+$ regulatory T (T_{reg}) cells, and normalized the dysregulated microbiota and metabolites in the small intestine in mouse models of food allergy. Inulin-gel-based OIT established immune tolerance with durable efficacy against repeated food allergen challenges. As inulin is a widely consumed dietary fibre that is generally recognized as safe by the FDA, our work shows the therapeutic and translational potential of inulin-gel-based OIT.

Gel formulation protects mice against allergen challenges

Inulin gel/allergen is formulated by a simple heating–cooling process with inulin in phosphate-buffered saline (PBS), followed by blending with protein allergens (Fig. 1a)—a streamlined procedure amenable to large-scale production and quality control. We first examined the efficacy of inulin gel/allergen in a widely used mouse model of anaphylaxis induced by chicken egg white ovalbumin (OVA)[21]. BALB/c mice were intraperitoneally sensitized with alum/OVA, followed by inulin gel/OVA OIT for 20 days (Fig. 1b). Inulin gel/OVA OIT-treated mice exhibited a good safety profile without any observable body-weight change, anaphylaxis or abnormal complete blood count and biochemistry (Extended Data Fig. 1). OIT-treated mice were subsequently subjected to repeated intragastric challenges with OVA protein, as repeated intragastric challenges increase the severity of oral-antigen-induced anaphylaxis[22]. After the sixth OVA challenge, mice in both PBS and free OVA groups exhibited a pronounced shock response as shown by the rapid drop in body temperature (Fig. 1c). In stark contrast, inulin gel/OVA markedly prevented systemic hypothermia (Fig. 1c), attenuated the anaphylactic response and allergic diarrhoea (Fig. 1d–g) and alleviated the body-weight drop (Fig. 1h). Inulin gel/OVA OIT prevented mortality in 100% mice from the repeated challenges, compared with the death rate of 19% and 31% in the OVA and PBS groups, respectively (Supplementary Fig. 1). In particular, inulin gel alone without the allergen showed no protective effect against repeated challenges (Extended Data Fig. 2), indicating the importance of co-formulating inulin gel with allergen. Moreover, the therapeutic efficacy was dependent on the degree of polymerization (DP) of inulin, as inulin gel/OVA composed of DP23 inulin showed improved protection against repeated OVA challenges and decreased the mast cell counts in the jejunum, compared with shorter DP inulin formulations, including inulin (DP7)/OVA or inulin gel (DP10)/OVA (Extended Data Fig. 3). Based on these results, we have used inulin gel (DP23) throughout the remaining studies. The mitigation of anaphylactic responses after inulin gel/OVA OIT was associated with decreased levels of OVA-specific IgE (known as the key indicator of anaphylaxis[23]), mucosal mast cell protease-1 (MMCP-1, a hallmark of mucosal mast cell degranulation[24]) and mast cells in the jejunum after the sixth intragastric challenge (Fig. 1i–k and Supplementary Fig. 2). Cytokine analysis of splenocytes restimulated ex vivo with OVA revealed that inulin gel/OVA elicited T_H1-skewed response with increased levels of IFNγ; increased ratios of IFNγ/IL-4, IFNγ/IL-5, IL-2/IL-4 and TNF/IL-5; and decreased T_H2 cytokines, including IL-4 and IL-13, compared with the PBS control (Fig. 1l–n). This allergen-specific shift of T_H2- to T_H1-type cytokines is known to dampen food allergic responses[14].

Engineered inulin gel is crucial for the efficacy of OIT

Previous studies have shown that mouse chow diet supplemented with free native inulin partially relieved allergic responses induced by a single intragastric allergen challenge[25]. Thus, we compared the efficacy of inulin gel/OVA against native inulin mixed with OVA (designated as inulin/OVA). Inulin/OVA OIT initially showed a protective effect on OVA challenge with mild anaphylactic and diarrhoea responses, but this effect was lost after repeated OVA challenges (Fig. 2a–c). Indeed, after the sixth challenge, mice treated with inulin/OVA developed severe hypothermic shock with significant body-weight loss, and 25% mice were dead (Fig. 2a–c). By contrast, inulin gel/OVA OIT resulted in improved protection throughout the six challenges (Fig. 2a–c). Compared with inulin/OVA, inulin gel/OVA OIT significantly decreased the levels of OVA-specific IgE and MMCP-1 in serum (Fig. 2d,e).

In particular, formulating inulin and OVA into gel increased its physical strength and viscosity (Fig. 2f). In vivo imaging studies demonstrated that the oral administration of Texas Red-labelled OVA formulated with fluorescein isothiocyanate (FITC)-labelled inulin gel significantly enhanced the retention of inulin gel (Supplementary Fig. 3) as well as OVA throughout the small intestine (Fig. 2g). In particular, inulin gel/OVA significantly enhanced the retention of OVA in the ileum, compared with the inulin/OVA group (Fig. 2h). Moreover, inulin gel/OVA OIT restored the intestinal barrier function, as shown by the decreased level of circulating FITC-dextran post-oral administration, compared with the inulin/OVA group (Fig. 2i). Furthermore, flow cytometry analysis revealed that inulin gel/OVA OIT facilitated antigen uptake by macrophage-like DCs (CD11c$^+$MHC-II^{high}CD103$^-$CX$_3$CR1$^+$ DCs; Fig. 2j) and recruited tolerogenic migratory DCs (CD11c$^+$MHC-II^{high}CD103$^+$CX$_3$CR1$^-$) into the small intestinal lamina propria (SI-LP) (Fig. 2k and Supplementary Fig. 4). Macrophage-like CX$_3$CR1$^+$ DCs are known to sample luminal antigens and transfer them to tolerogenic migratory CD103$^+$ DCs, which drive the differentiation of T_{reg} cells for oral tolerance induction[26].

Induction of immune regulatory cells in the small intestine

As the small intestine is known as a crucial site for immune tolerance against food antigens[14,16], we evaluated the immune landscape of the SI-LP after inulin gel/OVA OIT via single-cell RNA sequencing (scRNA-seq). Compared with free OVA, inulin gel/OVA OIT increased the frequencies of T_{reg} cells, T_H17 cells, IFNB1$^+$ DCs and cDC1 cells, whereas decreased plasma cells (Fig. 3a). In particular, compared with naive mice, OVA OIT substantially increased the frequencies of pathogenic mast cells and T_H2 cells, especially CD69$^+$ T_H2 cells (known to promote type 2 cytokines and allergen-specific IgE[27]), whereas inulin gel/OVA OIT decreased their frequencies (Fig. 3b). Overall, the scRNA-seq data indicated that inulin gel/OVA OIT restored the dysregulated immune cell subsets in allergic mice towards the 'healthy' status of naive mice.

Complementing these datasets, the flow cytometry analyses indicated that inulin gel/OVA OIT significantly decreased the frequency of pathogenic GATA3$^+$CD4$^+$ T_H2 cells but increased the frequency of

https://doi.org/10.1038/s41563-024-01909-w

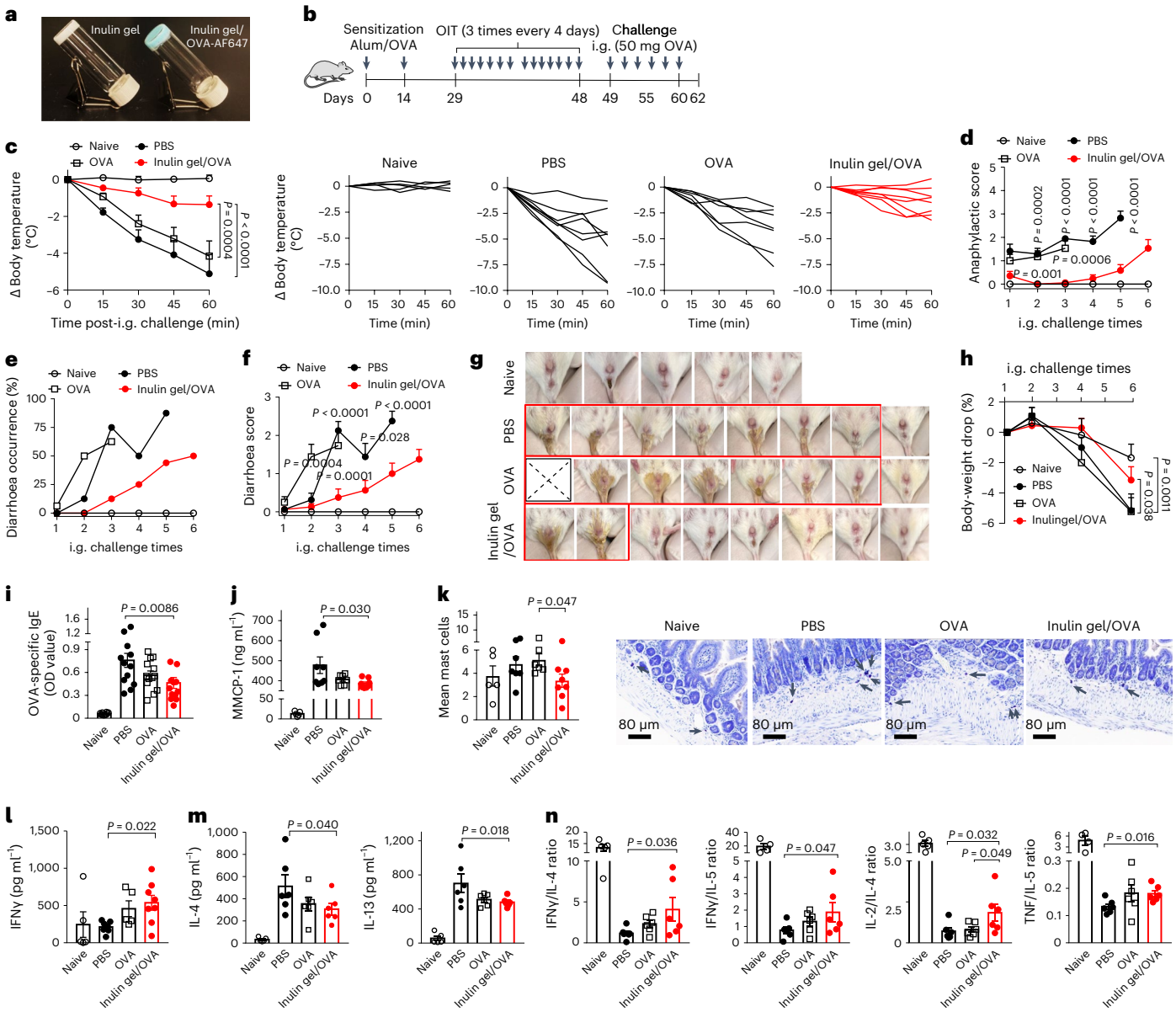

Fig. 1 | Inulin gel/OVA protects mice against repeated allergen challenges with chicken egg white. a, Images of inulin gel and inulin gel/AF647-labelled OVA. **b**, Schematic of the intestinal anaphylaxis and therapeutic regimen. As a healthy control group, naive BALB/c mice were not sensitized with alum/OVA. Mice in all other treatment groups were sensitized with alum/OVA on days 0 and 14. From day 29, alum/OVA-sensitized mice were orally gavaged with PBS, OVA (1 mg per dose) or inulin gel (55 mg per dose)/OVA (1 mg per dose) for three times every four days. From day 49, mice from all groups (including naive mice) were challenged intragastrically (i.g.) with OVA (50 mg per dose) on six alternating days (days 49, 51, 53, 56, 58 and 60). **c**, After the sixth intragastric challenge, changes in the average and individual core body temperature were measured. **d**–**h**, Over the six consecutive intragastric challenges, mice were analysed for anaphylactic scores (**d**), diarrhoea occurrence rate (**e**) and diarrhoea severity score (**f**); images of diarrhoea occurrence during the third intragastric challenge (red boundary marks mice with diarrhoea, and the X indicates mortality) (**g**); body-weight drop (**h**). **i**–**k**, Mice were analysed for serum-OVA-specific IgE levels on day 48 (**i**), serum MMCP-1 concentrations at 60 min after the sixth intragastric challenge on day 60 (**j**), mast cell counts (each dot represents one mouse) and toluidine blue staining of jejunal mast cells (arrows) on day 62 (**k**). **l**–**n**, Splenocytes were restimulated ex vivo with 250 μg ml^{-1} OVA on day 62. After 72 h, the supernatants were analysed for cytokines. The concentrations of IFNγ (**l**) and IL-4 and IL-13 (**m**) and the ratios of IFNγ/IL-4, IFNγ/IL-5, IL-2/IL-4 and TNF/IL-5 (**n**) are shown. Data represent mean ± s.e.m. from a representative experiment of two independent experiments ($n = 5$ for naive, 7 for OVA or 8 for PBS and inulin gel/OVA (**c**,**j**); $n = 10$ for naive or 17 for other groups (**d**,**h**); $n = 10$ for naive or 16 for other groups (**e**,**f**); $n = 10$ for naive or 13 for other groups (**i**); $n = 5$ for naive, 6 for OVA, 7 for PBS or 8 for inulin gel/OVA (**k**); $n = 5$ for naive and OVA, 7 for PBS or 8 for inulin gel/OVA (**l**); $n = 5$ for naive and 6 for other groups (**m**); $n = 5$ for naive in IFNγ/IL-4 and IL-2/IL-4 datasets and 4 for naive in IFNγ/IL-5 and TNF/IL-5 datasets; $n = 6$ for all other groups (**n**)). Data were analysed by two-way ANOVA (**c**,**d**,**f**,**h**) or one-way ANOVA (**i**–**n**) with Bonferroni's multiple comparisons test.

T-bet$^+$CD4$^+$ T_H1 cells in mesenteric lymph nodes (MLN) (Fig. 3c,d). Moreover, inulin gel/OVA OIT increased the frequencies of FOXP3$^+$CD4$^+$ T_{reg} cells in the SI-LP and MLN (Fig. 3e,f and Supplementary Figs. 5 and 6a). Further analysis on FOXP3$^+$CD4$^+$ T_{reg} cells revealed that inulin gel/OVA OIT reduced the frequency of T_H2-like GATA3$^+$CD4$^+$ T_{reg} cells (Fig. 3g) and promoted RORγt$^+$CD4$^+$ T_{reg} cells (Supplementary Fig. 6b). MLN cells analysed after ex vivo stimulation with phorbol 12-myristate 13-acetate (PMA) and ionomycin showed that inulin gel/OVA OIT increased the ratio of IFNγ$^+$CD4$^+$ T cells to IL-4$^+$CD4$^+$ T cells as well as IL-10 expression by T_H2 cells (Fig. 3h, i). Inulin gel/OVA OIT also increased the

https://doi.org/10.1038/s41563-024-01909-w

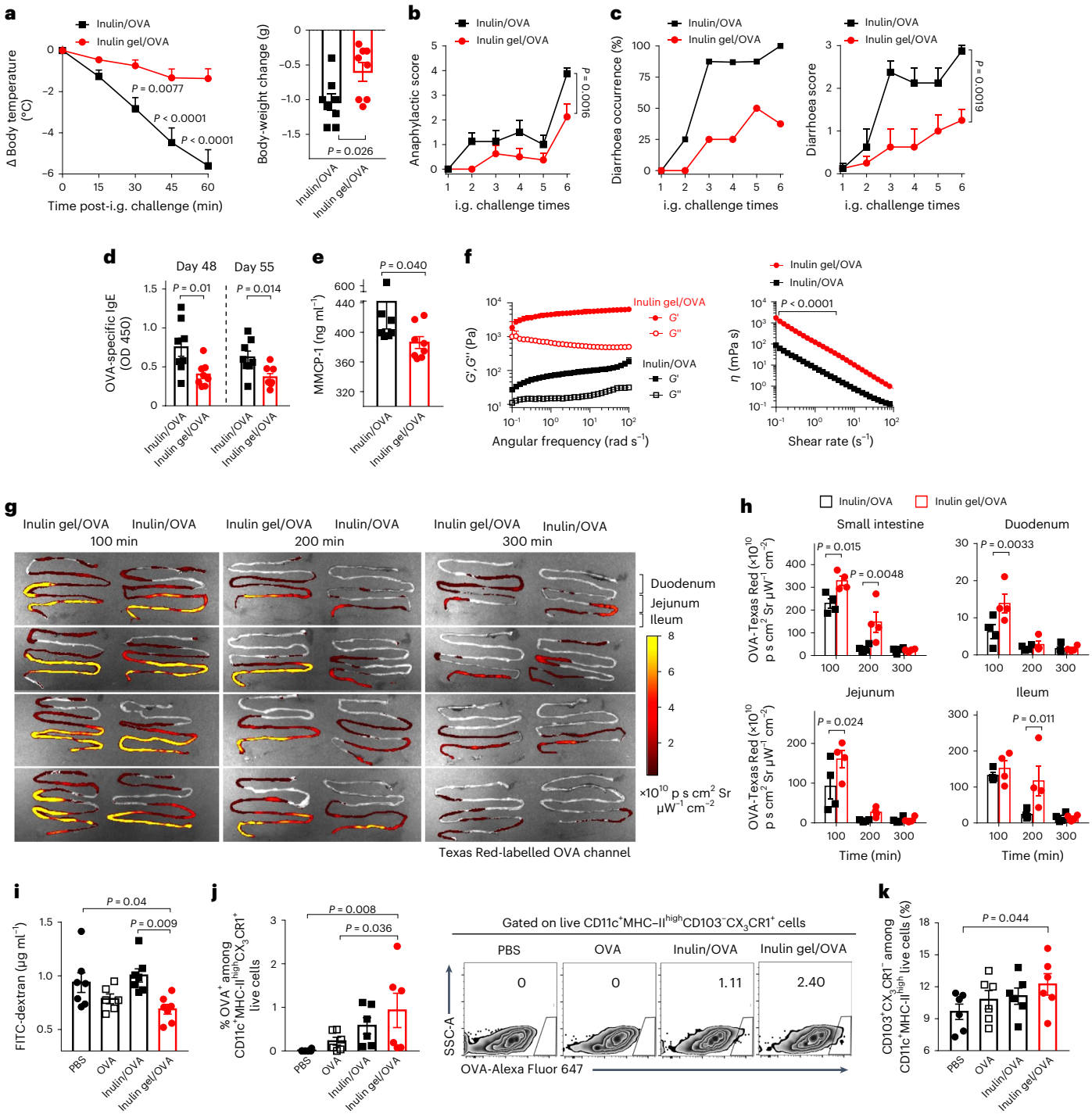

Fig. 2 | Inulin gel increases the residence time and uptake of allergen in the small intestine. Alum/OVA-sensitized BALB/c mice were treated as that shown in Fig. 1b. **a**, After the sixth intragastric challenge, the changes in the core body temperature and body weight were measured. **b**,**c**, Over the six consecutive intragastric challenges, anaphylactic scores (**b**) and diarrhoea occurrence rate and severity (**c**) were recorded. **d**,**e**, Mice were analysed with OVA-specific IgE levels in serum on days 48 and 55 (**d**) and the serum MMCP-1 concentration at 60 min post-intragastric challenge on day 60 (**e**). **f**, Dynamic rheological and viscosity measurements of inulin gel/OVA, inulin/OVA; *G′* (elastic modulus) and *G″* (viscous modulus). **g**,**h**, Alum/OVA-sensitized mice were orally gavaged with FITC-labelled inulin gel/Texas Red-labelled OVA, or FITC-labelled inulin/Texas Red-labelled OVA on day 29. The visualization of Texas Red-labelled OVA under Texas Red channel in the small intestine over time (**g**) and measurement of the total fluorescence intensity of Texas Red-labelled OVA in the small intestine, duodenum, jejunum and ileum (**h**) are shown. **i**, Mice were treated as in Fig. 1b and analysed for FITC-dextran in serum after oral gavage on day 57. **j**,**k**, Alum/OVA-sensitized BALB/c mice received OIT as in Fig. 1b. Mice were orally gavaged with inulin gel/AF647-labelled OVA or inulin/AF647-labelled OVA on day 49. After 3 h, the mice were euthanized for the analyses of OVA uptake by CX_3CR1^+ DCs (**j**) and frequency of $CD103^+$ DCs (**k**) in SI-LP via flow cytometry. Data represent the mean ± s.e.m. from one of two independent experiments ($n = 8$ (**a**–**d**), 3 (**f**), 4 (**h**) and 6 (**j**,**k**); $n = 7$ for inulin/OVA or 8 for inulin gel/OVA (**e**); $n = 6$ for OVA; or $n = 7$ for other groups (**i**) biologically independent samples). Data were analysed by two-way ANOVA (**a**–**c**,**f**,**h**) or one-way ANOVA (**i**–**k**) with Bonferroni's multiple comparisons test or two-tailed Mann–Whitney test (**e**) or unpaired, two-sided Student's *t*-test (**a**,**d**).

https://doi.org/10.1038/s41563-024-01909-w

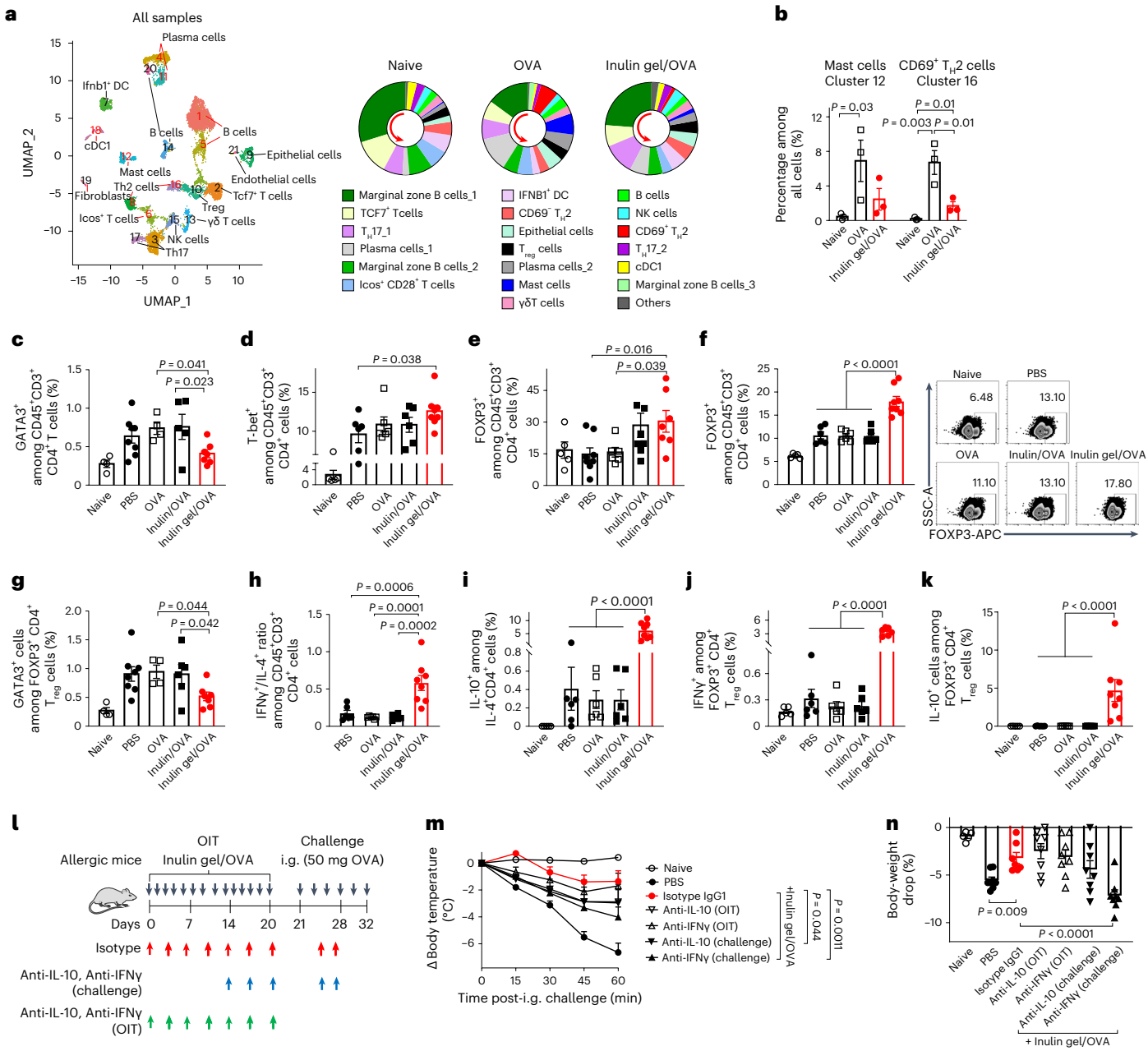

Fig. 3 | Inulin gel/OVA induces immune regulatory phenotype in the small intestine. BALB/c mice were treated as shown in Fig. 1b. The SI-LP were isolated on day 61, pooled from three mice per group and subjected to scRNA-seq. **a**,**b**, Uniform manifold approximation and projection (UMAP) in all samples, pie chart of the relative proportion of various cell types (**a**) and percentages of mast cells and CD69$^+$ T_H2 cells (**b**) were analysed. **c**–**g**, Small intestine and MLN were analysed before and after intragastric challenges. The frequencies of GATA3$^+$CD4$^+$ T_H2 cells on day 57 (**c**), T-bet$^+$CD4$^+$ T_H1 cells on day 61 (**d**) in MLN; FOXP3$^+$CD4$^+$ T_{reg} cells in SI-LP on day 49 (before the intragastric challenge; **e**), and in MLN on day 61 (**f**) and representative flow cytometry plots; and frequency of GATA3$^+$CD4$^+$ T_{reg} cells on day 57 (**g**) are shown. **h**–**k**, MLN cells were activated ex vivo with PMA and ionomycin on day 61. After 4 h, mice were analysed for the ratio of IFNγ$^+$/IL-4$^+$ in CD4$^+$ T cells (**h**), the frequencies of IL-10$^+$ among IL-4$^+$CD4$^+$ T cells (**i**), IFNγ$^+$ T_{reg} cells (**j**) and IL-10$^+$ T_{reg} cells (**k**). **l**–**n**, Alum/OVA-sensitized BALB/c mice were treated as in **l**, 100 μg of antibody against IL-10$^+$ cells, IFNγ$^+$ cells or isotype IgG1 control was administered intraperitoneally, as indicated. The changes in core body temperature (**m**) and body-weight drop at the sixth intragastric challenge (**n**) are shown. Data represent the mean ± s.e.m. ($n = 3$ (**b**); $n = 4$ for naive and OVA, 5 for inulin/OVA, 8 for PBS or 7 for inulin gel/OVA (**c**); $n = 5$ for naive, 8 for inulin gel/OVA or 6 for other groups (**d**,**f**,**i**–**k**); $n = 5$ for naive, 6 for OVA, 7 for inulin gel/OVA or 8 for other groups (**e**); $n = 4$ for naive and OVA, 6 for inulin/OVA, 8 for PBS or 7 for inulin gel/OVA (**g**); $n = 8$ for inulin gel/OVA or 6 for other groups (**h**); $n = 5$ for naive, 7 for PBS and inulin gel/OVA plus isotype IgG1, or 8 for other groups (**m**); $n = 5$ for naive, 7 for inulin gel/OVA plus isotype IgG1 or 8 for other groups (**n**)). Data were analysed by one-way ANOVA (**b**–**k**,**n**) or two-way ANOVA (**m**) with Bonferroni's multiple comparisons test.

expression of IFNγ and IL-10 among FOXP3$^+$CD4$^+$ T_{reg} cells (Fig. 3j,k)—subsets of T_{reg} cells known to suppress food allergy[28,29]. In line with these results, an in vitro co-culture study with bone-marrow-derived dendritic cells (BMDCs) and OT-II CD4$^+$ T cells showed that inulin gel/OVA markedly promoted the differentiation and proliferation of T_{reg} cells (Extended Data Fig. 4). Together, these data show that inulin gel/OVA OIT decreased T_H2-like cells whereas increased T_H1-type cells and T_{reg} cells in the SI-LP and MLN.

Next, we sought to delineate the role of T_{reg} cells and immune regulatory cytokines induced by inulin gel/OVA OIT. The administration of

anti-CD25 antibody abrogated the protective effects of inulin gel/OVA OIT (Supplementary Fig. 7), suggesting T_{reg} cell-mediated protection by inulin gel/OVA OIT. Specifically, we asked whether IFNγ and IL-10 exerted a protective role against the allergen challenge either by aiding with inulin gel/OVA-induced establishment of immune regulatory phenotype or by direct protection during allergen challenge. The administration of anti-IFNγ IgG or anti-IL-10 IgG during the challenge phase, but not during OIT, reversed protection by inulin gel/OVA (Fig. 3l–n). These results suggest that IFNγ and IL-10 secreted during the allergen challenge, rather than during the inulin-gel/OVA OIT, played a major role in immune protection.

In summary, these data indicated that inulin gel/OVA OIT shifted the T_H2-driven immune landscape in allergic mice towards T_H1- and T_{reg} cell-like phenotype and induced IFNγ$^+$ and IL-10$^+$ regulatory cells that protected animals against allergen challenge.

Inulin gel/OVA OIT establishes long-term protection

Palforzia requires initial dose escalation, up-dosing and maintenance dosing of allergen with a food vehicle. We mimicked this therapeutic regimen using inulin gel/OVA versus free OVA with dose escalation starting from 0.25 mg to a maintenance dose of 20 mg OVA (Fig. 4a). Over 75% of OVA-treated mice developed severe diarrhoea with marked body-weight decrease, and OVA-treated mice started to die after the third intragastric challenge (Fig. 4b–d). By contrast, inulin gel/OVA OIT inhibited anaphylactic responses and protected mice against diarrhoea (Fig. 4b–d). Inulin gel/OVA also reduced MMCP-1 in serum and mast cells in jejunum (Fig. 4e,f and Supplementary Fig. 8), and on ex vivo antigen restimulation, splenocytes from inulin gel/OVA group exhibited reduced T_H2 cytokine secretion with markedly lower levels of IL-4 and IL-9 (Fig. 4g).

We performed a re-challenge study after OIT cessation (Fig. 4a), as done in a clinical trial where sustained unresponsiveness was evaluated after the discontinuation of OIT[30]. Inulin gel/OVA OIT-protected mice against OVA re-challenge performed 30 days after OIT cessation, with 60% mice remaining free from diarrhoea (Fig. 4h). In line with this, mice treated with inulin gel/OVA maintained long-lasting immune tolerance profiles in the small intestine after OIT cessation; on day 79, mice still had significantly increased frequencies of FOXP3$^+$CD4$^+$ T_{reg} cells in SI-LP and CD103$^+$CD11C$^+$MHC-II$^+$ DCs in MLN; reduced frequency of IL-4$^+$FOXP3$^+$CD4$^+$ T_{reg} cells; and increased ratios of RORγt$^+$/GATA3$^+$, T-bet$^+$/GATA3$^+$, IFNγ$^+$/IL-4$^+$ among CD4$^+$ T cells and/or FOXP3$^+$CD4$^+$ T_{reg} cells in both SI-LP and MLN (Fig. 4i–m).

Insufficient maintenance dose during OIT can also increase the likelihood of regaining clinical reactivity[4]. To evaluate whether inulin gel/OVA can address this issue, we performed inulin gel/OVA OIT using a low dose of OVA (1 mg per dose), followed by oral challenges and OIT cessation. Surprisingly, even after 13 weeks of OIT cessation, mice treated with inulin gel/OVA OIT were well protected against repeated OVA re-challenges (Extended Data Fig. 5), indicating sustained unresponsiveness induced by the inulin gel/OVA OIT.

Restoration of dysregulated microbiota in ileum

To examine whether oral tolerance induced by inulin gel/OVA OIT was dependent on gut microbiota modulation, we orally administered broad-spectrum antibiotics to mice during inulin gel/OVA OIT, leading to the abrogation of the protective effects of inulin gel/OVA OIT (Fig. 5a,b).

In particular, the microbiome in the small intestine is thought to be crucial for the development of T_{reg} cells[16], mucosal immune system[31] and oral tolerance to food antigens[15]. In particular, within the small intestine, the ileum has the highest bacterial load and is associated with the largest mass of lymphoid tissue[16,31,32]. However, most food allergy studies have focused on the faecal microbiome, which is a proxy for the microbiota composition in the colon[12], rather than reflecting the dysregulated microbiota of the small intestine. Therefore, we examined microbial changes in both ileal and faecal contents during OIT via 16S ribosomal RNA gene sequencing. Consistent with other reports[8,31], the gut microbiota in the ileal contents showed significantly lower richness (operational taxonomic unit (OTU)) and α-diversity (inverse Simpson diversity values) than those in faeces (Fig. 5c). In the ileal contents, the non-metric multidimensional scaling analysis (NMDS; known as β diversity) revealed that OVA-treated mice showed high dissimilarities from naive mice ($P = 0.014$), whereas the microbial profile of inulin gel/OVA OIT-treated mice was overlapping with that of naive mice ($P = 0.48$; Fig. 5d). By contrast, the NMDS analysis of faecal microbiota revealed a distinct clustering of the microbial profiles of naive mice from all the treatment groups, including inulin gel/OVA OIT ($P < 0.001$; Fig. 5e).

In line with these results, microbial analyses at the family and genus levels indicated that OVA- and inulin/OVA-treated allergic mice had distinct ileal microbial profiles from that of naive mice, whereas inulin gel/OVA OIT restored the ileal microbiota to the 'normal' microbiome found in naive animals (Fig. 5f,g). By contrast, the faecal microbial community structure did not show any obvious shift among the different treatment groups (Fig. 5h,i).

Specifically, compared with naive mice, alum/OVA-sensitized mice treated with PBS, OVA or inulin/OVA had dramatically decreased the relative abundances of the *Eggerthellaceae* family and *Enterorhabdus* genus in the ileal contents, but not in the faecal contents (Fig. 5j). By contrast, inulin gel/OVA restored the relative abundances of both *Eggerthellaceae* and *Enterorhabdus* in the ileum to the normal levels in naive mice (Fig. 5j). We also performed Spearman's correlation coefficient analyses between the microbial abundances and serum-OVA-specific IgE titre. We observed an inverse correlation between the levels of OVA-specific IgE and the relative abundances of both *Eggerthellaceae* (family level, $r = -0.34$, $P = 0.04$) and *Enterorhabdus* (genus level, $r = -0.41$, $P = 0.013$) in the ileal contents, but not in the faeces ($r \approx 0$, $P \geq 0.83$; Fig. 5k,l). Interestingly, *Enterorhabdus* was recently reported to be negatively correlated with intestinal disorders[33,34]. In addition, inulin gel/OVA-treated mice had decreased ileal colonization of pathogenic *Helicobacter* and *Staphylococcus* (both known to be associated with food allergy and impaired oral tolerance[35,36]) as well as *Pelomonas* (associated with asthma, atopic dermatitis and allergen-specific IgE[37,38]) (Fig. 5g,k and Extended Data Fig. 6). Together, these data indicated the ileal microbiota as a crucial target of inulin gel/OVA OIT for food allergen desensitization.

Machine learning identifies immunomodulatory guanosine

We next examined changes in microbial metabolites in the ileal versus faecal contents during OIT via an untargeted metabolomics approach[39,40]. Sparse partial least-squares regression for discriminant analysis showed that the ileal contents from naive mice and inulin gel/OVA-treated mice had overlapping unbiased global metabolite profiles, whereas the ileal contents from naive mice had distinct metabolite profiles from PBS-, OVA- or inulin/OVA-treated mice (Extended Data Fig. 7a). By contrast, the faecal contents from naive mice showed distinct metabolite profiles from all the treatment groups, and the inulin gel/OVA and inulin/OVA groups had overlapping faecal metabolite profiles (Extended Data Fig. 7a,b and Supplementary Fig. 9). These untargeted metabolomics analyses, in line with the microbial analyses (Fig. 5), suggested that the therapeutic efficacy of inulin gel/OVA correlated with the restoration of the dysregulated microbiota and metabolites in ileum, rather than in faecal contents. Thus, we focused on analysing ileal metabolites after inulin gel/OVA OIT.

The metabolic pathway analysis in the ileal contents revealed that inulin gel/OVA OIT altered the metabolism of purine, pyrimidine, biotin and citric acid cycle (taurocholic acid cycle), compared with inulin/OVA OIT (Supplementary Fig. 10). In particular, inulin gel/OVA OIT substantially increased the ileal levels of nucleotides/nucleosides,

https://doi.org/10.1038/s41563-024-01909-w

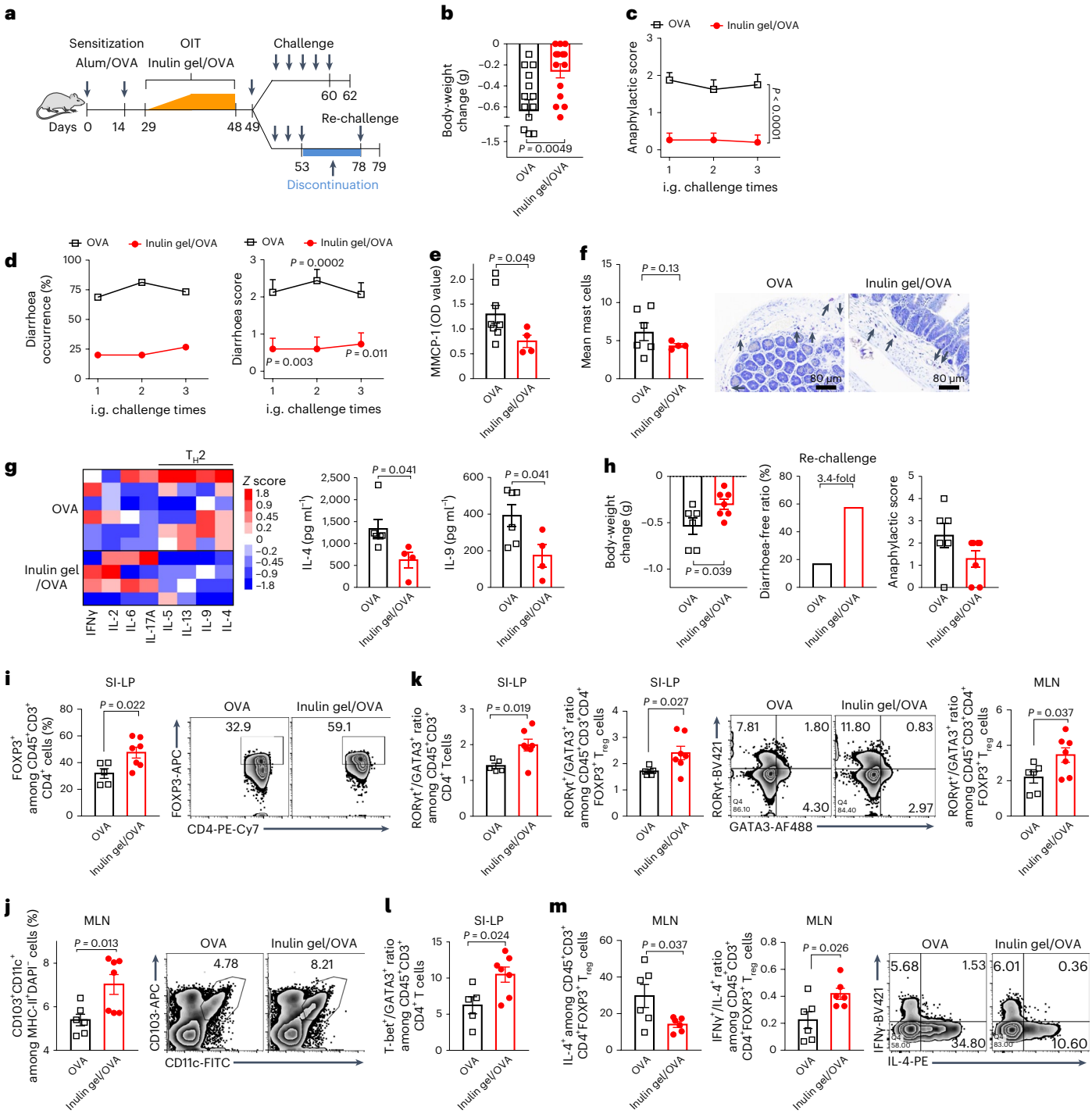

Fig. 4 | Inulin gel/OVA establishes durable protection with sustained unresponsiveness. a, Schematic of the intestinal anaphylaxis and therapeutic regimen. BALB/c mice were sensitized with alum/OVA. From day 29, mice were orally gavaged with inulin gel/OVA or free OVA. The dose of inulin gel was 55 mg, and the OVA (heated at 70 °C for 2 min) doses were 0.25, 0.5, 1, 2, 4, 8, 12 and 16 mg for the dose escalation phase and 20 mg for the maintenance phase. From day 49, mice were intragastric. challenged with OVA (50 mg per dose) on six alternating days (**b**–**g**) or challenged for four times and discontinued for 25 days, followed by intragastric re-challenge of OVA (**h**–**m**). **b**, After the third intragastric challenge, the body-weight change was recorded. **c**,**d**, During the three consecutive intragastric challenges, mice were analysed for anaphylactic scores (**c**) as well as diarrhoea occurrence rate and diarrhoea severity (**d**). **e**,**f**, Mice were analysed for MMCP-1 in serum on day 60 (**e**) and mast cell counts and toluidine blue staining of jejunal mast cells (arrows) on day 62 (**f**). **g**, Splenocytes were restimulated ex vivo with 250 μg ml^{-1} OVA on day 62. After 72 h, the supernatants were analysed for cytokines. **h**–**m**, Mice were re-challenged with OVA 25 days after the fourth intragastric challenge. Body-weight changes, anaphylactic scores and diarrhoea-free mice ratio on day 78 were measured (**h**); on day 79, mice were further analysed for the frequencies of FOXP3$^+$CD4$^+$ T_{reg} cells in SI-LP (**i**); CD103$^+$ DCs in MLN (**j**); the ratios of ROR-γt$^+$/GATA3$^+$ among CD4$^+$ T cells and FOXP3$^+$CD4$^+$ T_{reg} cells in SI-LP and MLN (**k**); the ratio of T-bet$^+$/GATA3$^+$ among CD4$^+$ T cells in SI-LP (**l**) and frequency of IL-4$^+$FOXP3$^+$CD4$^+$ T cells and ratio of IFNγ$^+$/IL-4$^+$ among FOXP3$^+$CD4$^+$ T_{reg} cells in MLN (**m**). Data represent the mean ± s.e.m. from a representative experiment of two independent experiments ($n = 15$ for OVA or 14 for inulin gel/OVA (**b**); $n = 16$ for OVA or 15 for inulin gel/OVA (**c**,**d**); $n = 8$ for OVA or 4 for inulin gel/OVA (**e**); $n = 6$ for OVA or 4 for inulin gel/OVA (**f**,**g**); $n = 6$ for OVA or 7 for inulin gel/OVA (**h**,**j**); $n = 5$ for OVA or 7 for inulin gel/OVA (**i** and **l**); $n = 5$ for OVA in SI-LP dataset and 6 for OVA in MLN dataset or 7 for inulin gel/OVA (**k**); $n = 6$ (**m**) biologically independent samples). Data were analysed by two-way ANOVA with Bonferroni's multiple comparisons test (**c**,**d**) or unpaired, one-sided Student's *t*-test (**f**) or two-tailed Mann–Whitney test (**e**) or unpaired, two-sided Student's *t*-test (**b**,**g**–**m**).

including guanosine, uridine, 5-thymidylic acid, pseudouridine, orotidine 5′-monophosphate and biotin whereas decreased the levels of guanosine-5′-diphosphate and phenylpropiolic acid, compared with at least three other groups (Extended Data Fig. 7b and Supplementary Fig. 9). Inulin gel/OVA OIT also increased the levels of ileal short-chain fatty acids (Supplementary Fig. 11). Specifically, among these metabolites, guanosine was markedly decreased in mice treated with PBS ($P < 0.01$), OVA ($P < 0.05$) or inulin/OVA ($P < 0.01$), but inulin gel/OVA OIT significantly increased its level by 50%, compared with PBS ($P < 0.05$) and inulin/OVA ($P < 0.05$), restoring it to the normal level found in naive mice (Extended Data Fig. 7b). It is intriguing that certain nucleosides, including guanosine, are known to be protective against neurodegenerative disorders[41], and guanosine has been shown to inhibit the MAPK and NF-κB pathways in M1 macrophages[42]; however, its effect on T cells is unknown. When we added guanosine to $CD4^+$ T cell culture in suboptimal T_{reg}- or T_H1 cell-inducing conditions, guanosine significantly increased $FOXP3^+CD25^+$ T_{reg} cells and $IFN\gamma^+CD4^+$ T cells, respectively (Extended Data Fig. 7c,d). Moreover, even in a T_H2-inducing condition, guanosine treatment substantially increased the frequency of $IFN\gamma^+CD4^+$ T cells in a dose-dependent manner (Extended Data Fig. 7e). By contrast, we did not observe such T_{reg}- or T_H1 cell-skewed responses with other metabolites that were increased in the ileum after inulin gel/OVA OIT, including 5-thymidylic acid, acetic acid, propionic acid, butyric acid, uridine, biotin and 2′-deoxyguanosine (a chemical derivative of guanosine) (Extended Data Fig. 7c–e). Additionally, guanosine co-cultured with BMDCs in the presence of lipopolysaccharide decreased the expressions of CD80 and CD86 on $CD11c^+CD11b^{int}MHC\text{-}II^{hi}$ DCs, compared with lipopolysaccharide treatment alone (Supplementary Fig. 12). To examine whether guanosine contributed to oral tolerance in vivo, we provided mice with or without guanosine in drinking water during OVA OIT. In response to repeated OVA challenges, OVA/guanosine OIT markedly attenuated the drop in body temperature, anaphylactic shock and diarrhoea, compared with OVA alone, although to a less degree than inulin gel/OVA OIT (Extended Data Fig. 8). Together, these results suggest that inulin gel/OVA OIT increased the ileal level of guanosine, which can tip the balance of T_H2 phenotype to T_H1 and T_{reg} cell phenotypes, thereby contributing to the protective effects of inulin gel/OVA OIT.

The recent pioneering studies have integrated metabolomics in the microbiome analyses, most particularly, the NIH Human Microbiome Project that focused on inflammatory bowel disease and prediabetes[43]. However, the correlation between the ileal microbiome and metabolome in food allergy and OIT remains unknown. We sought to delineate their association in the ileum using the hierarchical all-against-all significance association (HAllA) machine learning algorithm[44], based on datasets obtained from the same animals. The HAllA algorithm can identify highly general association types in paired, high-dimensional and heterogeneous datasets with a high statistical power. We first separately performed hierarchical clustering within the microorganisms and the metabolite datasets to generate two data hierarchies in the order of similarity (Extended Data Fig. 7f (family level) and Supplementary Fig. 13 (genus level)). The machine learning analysis indicated a highly positive association between guanosine and *Eggerthellaceae* at the family level (Extended Data Fig. 7f) and *Enterorhabdus* and *Eggerthellaceae_unclassified* at the genus level (Supplementary Fig. 13). Indeed, Spearman's correlation analysis indicated statistically significant correlation between guanosine and *Eggerthellaceae* as well as *Enterorhabdus* in the ileum ($P < 0.01$; Extended Data Fig. 7g)—in line with a recent report[45]. These data suggest that inulin-gel-based OIT modulates the ileal microbiota, leading to the normalization of the dysregulated microbiome and metabolites, including guanosine, which contribute to immune regulatory responses against food allergy.

Efficacy in various food allergy models

We sought to validate the efficacy of the inulin/allergen OIT in various food allergy models. Inulin gel/casein OIT efficiently protected BALB/c mice in a model of cow's milk allergy (Fig. 6a–c). Similarly, inulin gel/peanut extract OIT-protected C3H/HeJ mice against peanut allergy in alum/allergen-sensitized, oral-antigen-induced anaphylaxis (Fig. 6d–f). In addition, we sensitized mice with oral cholera toxin/peanut extract, followed by OIT and intraperitoneal peanut extract challenge (Fig. 6g). Cholera toxin can break oral tolerance, while parenteral peanut extract challenge induces more serious symptoms than the oral route. Mice treated with inulin gel/peanut extract were protected against the peanut extract challenge, as shown by the significantly decreased drops in body temperature (Fig. 6h,i) and anaphylactic responses (Fig. 6j). Moreover, a shorter and less-frequent regimen (inulin gel/OVA OIT every other day for 12 days) also protected mice against repeated OVA challenges (Extended Data Fig. 9). Together, inulin gel/allergen OIT was effective in various food allergy models in multiple mouse strains that exhibit different genetic predispositions, gut microbiome and immunological status[46,47].

Safety and tolerability of inulin gel/OVA OIT

A recent study reported that mice on a chow diet supplemented with 26% inulin fibre exhibited signs of type 2 inflammation, including eosinophilia in the colon and lungs and increased microbiota-derived bile acids[48]. Thus, we compared the impact of a high inulin diet (26% inulin, equivalent to ~1,040 mg inulin consumption per day) versus inulin gel treatments used in the current study (55 mg dose per day). Indeed, naive mice kept on a high (26%) inulin diet for 13 days markedly increased eosinophils, neutrophils and monocytes in the colon (Extended Data Fig. 10a–i), compared with mice on a normal control diet. A high inulin diet also increased the levels of cholic acid and taurocholic acid in serum, decreased levels of ω-muricholic acid and deoxycholic acid in faeces, and ω-muricholic acid and chenodeoxycholic acid in caecum (Extended Data Fig. 10j–l). In stark contrast, naive mice treated with 55 mg inulin or inulin gel showed normal levels of various immune cell subsets (that is, eosinophils, neutrophils, monocytes, macrophages,

Fig. 5 | Inulin gel/OVA normalizes the dysbiotic ileal microbiota in food allergy. a,**b**, Alum/OVA-sensitized mice were fed with antibiotic cocktails during OIT. From day 49, the mice received repeated intragastric challenges of OVA. **a**, Over the four consecutive intragastric challenges, changes in the anaphylactic scores, diarrhoea occurrence rate and diarrhoea severity were measured. **b**, After the fourth challenge, the body-weight changes were recorded. **c**–**l**, Alum/OVA-sensitized BALB/c mice were treated as that shown in Fig. 1b. The microbial communities in the ileal contents and faeces were analysed via 16S rRNA gene sequencing. The analyses of the observed OTU, inverse Simpson diversity (**c**); the NMDS score plot (based on Bray–Curtis) in the ileal contents (**d**) and faeces (**e**); the relative abundances of the gut commensal microorganisms at the phylum and family levels in the ileal contents (**f**) and faeces (**h**); the heat maps showing the normalized *Z*-score values of the relative abundances of differentially abundant microorganisms at genus level in the ileal contents (**g**) and faeces (**i**) are shown. **j**, Relative abundances of *Eggerthellaceae* and *Enterorhabdus* in the ileal contents and faeces were compared. **k**, Spearman's correlation coefficient analyses between the level of OVA-specific IgE in serum and the relative abundances of various differentially abundant microorganisms in the ileal contents or faeces. **l**, Spearman's correlation coefficient analyses of *Eggerthellaceae* and *Enterorhabdus* with OVA-specific IgE in the ileal contents and faeces were compared. p, phylum; f, family; g, genus. Data represent the mean ± s.e.m. ($n = 5$ (**a**,**b**); $n = 5$ for naive, 7 for OVA in ileal contents dataset or inulin/OVA in the faeces dataset or 8 for all other groups (**c**–**e**,**j**) biologically independent samples). Data were analysed by an analysis of molecular variance (AMOVA) (**d**,**e**); one-way (**c**,**j**) or two-way (**a**) ANOVA with Bonferroni's multiple comparisons test or unpaired, two-sided Student's *t*-test (**b**); or two-tailed Spearman's rank correlation test (**k**,**l**). NS, not significant.

https://doi.org/10.1038/s41563-024-01909-w

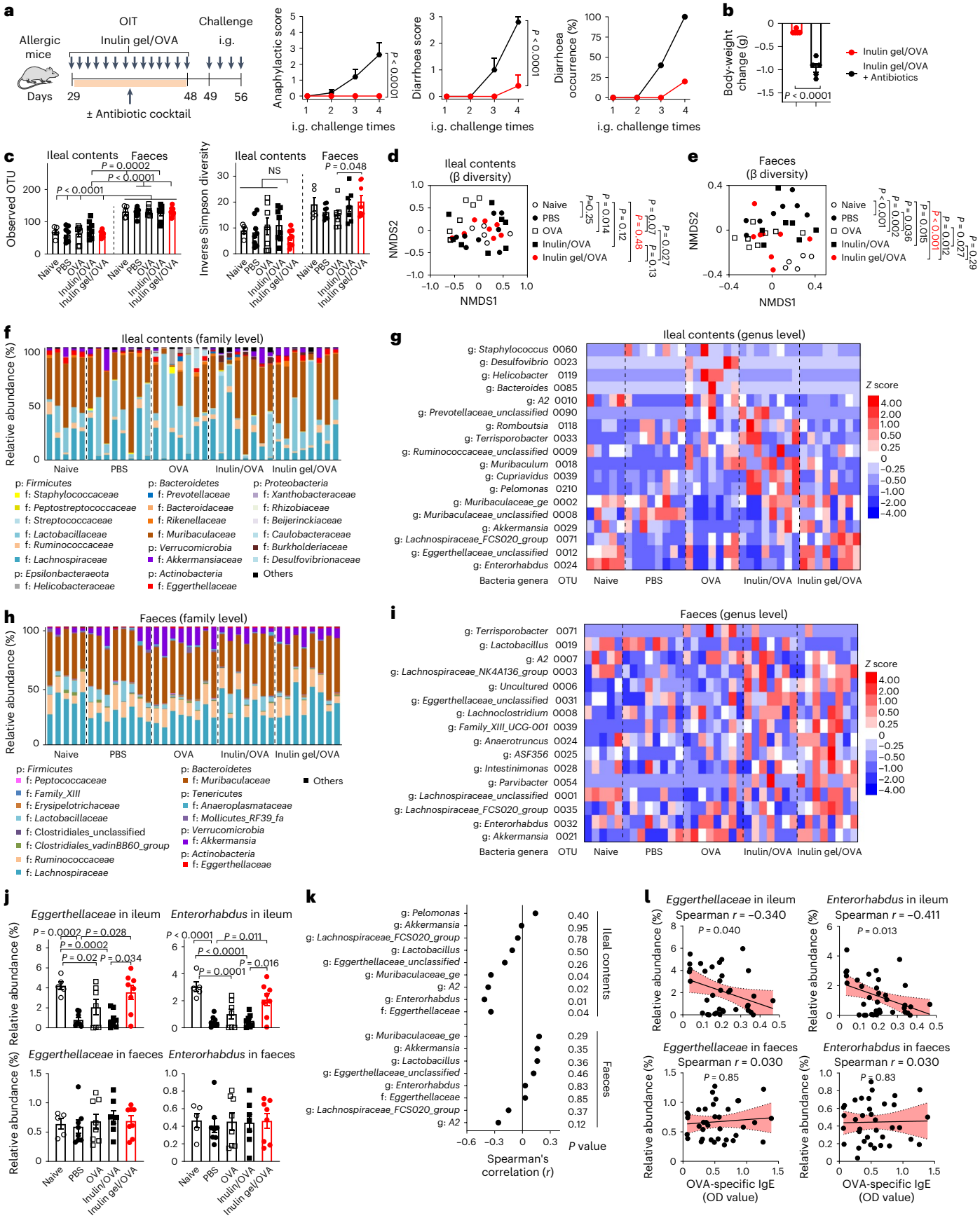

https://doi.org/10.1038/s41563-024-01909-w

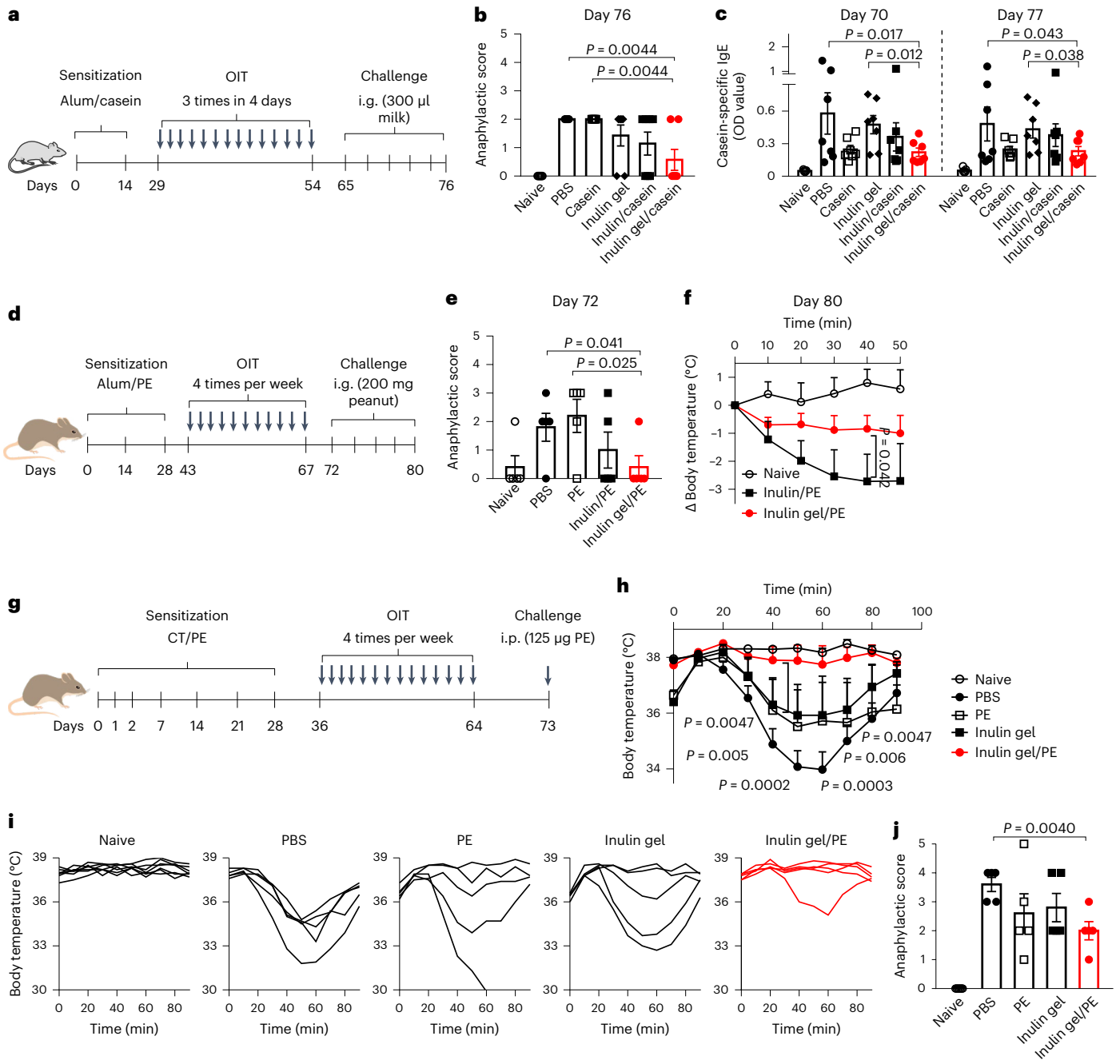

Fig. 6 | Therapeutic efficacy of inulin gel/allergen OIT in various food allergy models. a, Therapeutic regimen of cow's milk allergy in BALB/c mice (**a**). **b**,**c**, Mice were analysed for anaphylactic scores on day 76 (**b**) and casein-specific IgE in serum on days 70 and 77 (**c**). **d**, Therapeutic regimen of peanut allergy in alum/peanut extract (PE)-sensitized C3H/HeJ mice with intragastric challenges. **e**,**f**, Mice were analysed for anaphylactic scores on day 72 (**e**) and changes in the average core body temperature (**f**) after repeated intragastric challenges of peanut powder. **g**, Therapeutic regimen of peanut allergy in cholera toxin/peanut extract (CT/PE)-sensitized C3H/HeJ mice. **h**–**j**, Parenteral antigen-induced anaphylaxis (**g**), changes in the average (**h**) and individual core body temperature (**i**), and anaphylactic scores (**j**) after intraperitoneal challenge of peanut extract were measured. Data represent the mean ± s.e.m. from a representative experiment of two independent experiments ($n = 5$ for naive or 7 for all other groups (**b**,**c**); $n = 5$ (**e**,**f**); $n = 7$ for naive or 5 for all other groups (**h**–**j**) biologically independent samples). Data were analysed by two-way (**f**,**h**) or one-way (**b**,**c**,**e**,**j**) ANOVA with Bonferroni's multiple comparisons test.

DCs, B cells and T cells) in the colon and lungs as well as bile acids in serum, colon and caecum (Extended Data Fig. 10). Moreover, inulin gel/OVA OIT did not induce any signs of type 2 inflammation in allergic mice (Supplementary Figs. 14 and 15). Together, our low-dose inulin gel was well tolerated in healthy or allergic mice without any major safety concerns.

In summary, we have developed a new dietary-fibre-based gel platform that can induce tolerogenic intestinal mucosal environment and establish long-term protection against food allergy. Our therapeutic strategy is based on a simple oral formulation of allergen and inulin with FDA generally recognized as safe status, thereby potentially expediting scale-up manufacturing and translation. Moreover, our work reveals the diversity of gut microbiota and metabolites along the gastrointestinal tract after OIT and provides new insights into the interplay among gut homoeostasis, immune profiles and food allergy. As dysregulated microbiome and metabolites are linked to various

autoimmune and allergic diseases, our strategy may offer a general pathway for microbiome-modulating therapeutic interventions.

Online content

Any methods, additional references, Nature Portfolio reporting summaries, source data, extended data, supplementary information, acknowledgements, peer review information; details of author contributions and competing interests; and statements of data and code availability are available at https://doi.org/10.1038/s41563-024-01909-w.

References

1. Sicherer, S. H. Food allergy. *Lancet* **360**, 701–710 (2002).
2. Mullard, A. FDA approves first peanut allergy drug. *Nat. Rev. Drug Discov.* **19**, 156 (2020).
3. Brown, K. R. et al. Safety of peanut (*Arachis hypogaea*) allergen powder-dnfp in children and teenagers with peanut allergy: pooled summary of phase 3 and extension trials. *J. Allergy Clin. Immunol.* **149**, 2043–2052. e2049 (2022).
4. Chinthrajah, R. S. et al. Sustained outcomes in oral immunotherapy for peanut allergy (POISED study): a large, randomised, double-blind, placebo-controlled, phase 2 study. *Lancet* **394**, 1437–1449 (2019).
5. Stephen-Victor, E., Crestani, E. & Chatila, T. A. Dietary and microbial determinants in food allergy. *Immunity* **53**, 277–289 (2020).
6. Abdel-Gadir, A. et al. Microbiota therapy acts via a regulatory T cell MyD88/RORγt pathway to suppress food allergy. *Nat. Med.* **25**, 1164–1174 (2019).
7. Iweala, O. I. & Nagler, C. R. The microbiome and food allergy. *Annu. Rev. Immunol.* **37**, 377–403 (2019).
8. Stefka, A. T. et al. Commensal bacteria protect against food allergen sensitization. *Proc. Natl Acad. Sci. USA* **111**, 13145–13150 (2014).
9. Hwang, D. W., Nagler, C. R. & Ciaccio, C. E. New and emerging concepts and therapies for the treatment of food allergy. *Immunother. Adv.* **2**, ltac006 (2022).
10. Tan, J. et al. Dietary fiber and bacterial SCFA enhance oral tolerance and protect against food allergy through diverse cellular pathways. *Cell Rep.* **15**, 2809–2824 (2016).
11. Vasapolli, R. et al. Analysis of transcriptionally active bacteria throughout the gastrointestinal tract of healthy individuals. *Gastroenterology* **157**, 1081–1092. e1083 (2019).
12. Lkhagva, E. et al. The regional diversity of gut microbiome along the GI tract of male C57BL/6 mice. *BMC Microbiol.* **21**, 44 (2021).
13. Yuan, C., Graham, M., Staley, C. & Subramanian, S. Mucosal microbiota and metabolome along the intestinal tract reveal a location-specific relationship. *mSystems* **5**, e00055-20 (2020).
14. Yu, W., Freeland, D. M. H. & Nadeau, K. C. Food allergy: immune mechanisms, diagnosis and immunotherapy. *Nat. Rev. Immunol.* **16**, 751–765 (2016).
15. Feehley, T. et al. Healthy infants harbor intestinal bacteria that protect against food allergy. *Nat. Med.* **25**, 448–453 (2019).
16. Shan, M. et al. Mucus enhances gut homeostasis and oral tolerance by delivering immunoregulatory signals. *Science* **342**, 447–453 (2013).
17. Woting, A. & Blaut, M. Small intestinal permeability and gut-transit time determined with low and high molecular weight fluorescein isothiocyanate-dextrans in C3H mice. *Nutrients* **10**, 685 (2018).
18. Caride, V. et al. Scintigraphic determination of small intestinal transit time: comparison with the hydrogen breath technique. *Gastroenterology* **86**, 714–720 (1984).
19. Chehade, M. & Mayer, L. Oral tolerance and its relation to food hypersensitivities. *J. Allergy Clin. Immunol.* **115**, 3–12 (2005).
20. Han, K. et al. Generation of systemic antitumour immunity via the in situ modulation of the gut microbiome by an orally administered inulin gel. *Nat. Biomed. Eng.* **5**, 1377–1388 (2021).
21. Osterfeld, H. et al. Differential roles for the IL-9/IL-9 receptor α-chain pathway in systemic and oral antigen–induced anaphylaxis. *J. Allergy Clin. Immunol.* **125**, 469–476.e462 (2010).
22. Ahrens, R. et al. Intestinal mast cell levels control severity of oral antigen-induced anaphylaxis in mice. *Am. J. Pathol.* **180**, 1535–1546 (2012).
23. Jones, S. M. & Burks, A. W. Food allergy. *N. Engl. J. Med.* **377**, 1168–1176 (2017).
24. Galand, C. et al. IL-33 promotes food anaphylaxis in epicutaneously sensitized mice by targeting mast cells. *J. Allergy Clin. Immunol.* **138**, 1356–1366 (2016).
25. Wagenaar, L. et al. Dietary supplementation with nondigestible oligosaccharides reduces allergic symptoms and supports low dose oral immunotherapy in a peanut allergy mouse model. *Mol. Nutr. Food Res.* **62**, 1800369 (2018).
26. Mazzini, E., Massimiliano, L., Penna, G. & Rescigno, M. Oral tolerance can be established via gap junction transfer of fed antigens from CX_3CR1^+ macrophages to $CD103^+$ dendritic cells. *Immunity* **40**, 248–261 (2014).
27. Wang, S. H. et al. An exhausted phenotype of TH2 cells is primed by allergen exposure, but not reinforced by allergen-specific immunotherapy. *Allergy* **76**, 2827–2839 (2021).
28. Huang, C.-H., Wang, C.-C., Lin, Y.-C., Hori, M. & Jan, T.-R. Oral administration with diosgenin enhances the induction of intestinal T helper 1-like regulatory T cells in a murine model of food allergy. *Int. Immunopharmacol.* **42**, 59–66 (2017).
29. Hong, J. Y. et al. Frontline science: TLR3 activation inhibits food allergy in mice by inducing IFN-γ^+ $Foxp3^+$ regulatory T cells. *J. Leukoc. Biol.* **106**, 1201–1209 (2019).
30. Burks, A. W. et al. Oral immunotherapy for treatment of egg allergy in children. *N. Engl. J. Med.* **367**, 233–243 (2012).
31. Kastl, A. J. Jr, Terry, N. A., Wu, G. D. & Albenberg, L. G. The structure and function of the human small intestinal microbiota: current understanding and future directions. *Cell. Mol. Gastroenterol. Hepatol.* **9**, 33–45 (2020).
32. El Aidy, S., Van Den Bogert, B. & Kleerebezem, M. The small intestine microbiota, nutritional modulation and relevance for health. *Curr. Opin. Biotechnol.* **32**, 14–20 (2015).
33. Wang, K. et al. Gut microbiota disorder caused by diterpenoids extracted from *Euphorbia pekinensis* aggravates intestinal mucosal damage. *Pharmacol. Res. Perspect.* **9**, e00765 (2021).
34. Ma, L. et al. Xuanfei Baidu decoction attenuates intestinal disorders by modulating NF-κB pathway, regulating T cell immunity and improving intestinal flora. *Phytomedicine* **101**, 154100 (2022).
35. Ling, Z. et al. Altered fecal microbiota composition associated with food allergy in infants. *Appl. Environ. Microbiol.* **80**, 2546–2554 (2014).
36. Matysiak-Budnik, T. et al. Gastric *Helicobacter* infection inhibits development of oral tolerance to food antigens in mice. *Infect. Immun.* **71**, 5219–5224 (2003).
37. Chen, M. et al. Nasal bacterial microbiome differs between healthy controls and those with asthma and allergic rhinitis. *Front. Cell. Infect. Microbiol.* **12**, 841995 (2022).
38. Riskumäki, M. et al. Interplay between skin microbiota and immunity in atopic individuals. *Allergy: Eur. J. Allergy. Clin. Immunol.* **76**, 1280–1284 (2021).
39. Achreja, A. et al. Metabolic collateral lethal target identification reveals MTHFD2 paralogue dependency in ovarian cancer. *Nat. Metab.* **4**, 1119–1137 (2022).
40. Zhu, Z. et al. Tumour-reprogrammed stromal BCAT1 fuels branched-chain ketoacid dependency in stromal-rich PDAC tumours. *Nat. Metab.* **2**, 775–792 (2020).
41. Bettio, L. E., Gil-Mohapel, J. & Rodrigues, A. L. S. Guanosine and its role in neuropathologies. *Purinergic Signal.* **12**, 411–426 (2016).

42. Luo, Y. et al. Guanosine and uridine alleviate airway inflammation via inhibition of the MAPK and NF-κB signals in OVA-induced asthmatic mice. *Pulm. Pharmacol. Ther.* **69**, 102049 (2021).
43. The Integrative HMP (iHMP) Research Network Consortium. The integrative human microbiome project. *Nature* **569**, 641–648 (2019).
44. Rahnavard, G. et al. High-sensitivity pattern discovery in large multi'omic datasets. https://huttenhower.sph.harvard.edu/halla (2017).
45. Zhang, H., Hui, X., Wang, Y. & Lu, X. Angong Niuhuang Pill ameliorates cerebral ischemia/reperfusion injury in mice partly by restoring gut microbiota dysbiosis. *Front. Pharmacol.* **13**, 1001422 (2022).
46. Morafo, V. et al. Genetic susceptibility to food allergy is linked to differential TH2-TH1 responses in C3H/HeJ and BALB/c mice. *J. Allergy Clin. Immunol.* **111**, 1122–1128 (2003).
47. Wagenaar, L. et al. Mouse strain differences in response to oral immunotherapy for peanut allergy. *Immun. Inflamm. Dis.* **7**, 41–51 (2019).
48. Arifuzzaman, M. et al. Inulin fibre promotes microbiota-derived bile acids and type 2 inflammation. *Nature* **611**, 578–584 (2022).

[1]Department of Pharmaceutical Sciences, University of Michigan, Ann Arbor, MI, USA. [2]Biointerfaces Institute, University of Michigan, Ann Arbor, MI, USA. [3]Department of Biomedical Engineering, University of Michigan, Ann Arbor, MI, USA. [4]Department of Chemical Engineering, University of Michigan, Ann Arbor, MI, USA. [5]Division of Gastroenterology, Department of Internal Medicine, University of Michigan, Ann Arbor, MI, USA. [6]Graduate Program in Biostatistics, University of Washington, Seattle, WA, USA. [7]Departments of Head and Neck Surgery and of Cancer Biology, the University of Texas M.D. Anderson Cancer Center, Houston, TX, USA. [8]Department of Biomedical Engineering, Dongguk University, Seoul, Republic of Korea. [9]Mary H. Weiser Food Allergy Center, University of Michigan, Ann Arbor, MI, USA. [10]Department of Computational Mathematics, Science and Engineering, Michigan State University, East Lansing, MI, USA. [11]Department of Statistics and Probability, Michigan State University, East Lansang, MI, USA. [12]WPI Immunology Frontier Research Center, Osaka University, Suita, Japan. [13]Present address: State Key Laboratory of Natural Medicines and Jiangsu Key Laboratory of Drug Design and Optimization, Department of Pharmaceutics, China Pharmaceutical University, Nanjing, China. [14]These authors contributed equally: Kai Han, Fang Xie. ✉e-mail: moonjj@umich.edu

Methods

Preparation and characterization of inulin gel/allergen formulations

For inulin gel/OVA or inulin gel/casein, 495 mg of inulin was dissolved in 1.35 ml PBS and heated at 70 °C for 5 min with shaking. Then, 9 mg of OVA (Grade V, Sigma-Aldrich), casein (from bovine milk, 87–94% protein basis, Sigma-Aldrich) or preset dose of OVA was added right after cool-down of the inulin solution. For inulin gel/PE, 300 mg of inulin was dissolved in 0.9 ml deionized water. After heating for 5 min, 8 mg of PE was added right after cool-down of the inulin solution. All these samples were kept at 4 °C for 24 h to get the inulin gel/allergen formulations. PE was prepared as described in a previous report with a minor modification[49]. In brief, 40 g of raw peanut powder was added to 500 ml of deionized water and stirred for 2 h at room temperature. The suspension was sonicated for 15 min and centrifuged at 3,000*g* for 30 min. Then, the supernatant was carefully collected and further centrifuged at 8,000*g* for 60 min. The supernatant containing the protein was lyophilized. The protein content in PE (around 20%) was determined by a bicinchoninic acid assay (Thermo Fisher). The rheology study of inulin gel/OVA was carried out according to manufacturer's instruction (Anton Parr MCR702 rheometer).

In vivo sensitization, OIT and challenges

Animals were cared for following the federal, state and local guidelines. All work conducted on animals were in accordance with and approved by the Institutional Animal Care and Use Committee. Female C3H/HeJ mice or BALB/c (5–6 weeks old) from Jackson Laboratory were fed on the mouse chow diet (PicoLab Laboratory Rodent Diet 5L0D*). Mice were acclimatized for 1 week before experiment, followed by co-housing during the sensitization. For alum/OVA model, BALB/c mice were injected intraperitoneally with OVA (50 μg per dose) and alum (1 mg per dose, aluminium hydroxide gel, Invivogen) in 150 μl PBS on days 0 and 14. Naive mice not sensitized to OVA were included as a non-allergic, healthy control. The alum/OVA-sensitized mice were randomly grouped on day 28. From day 29, the sensitized mice were orally administered with PBS, OVA, inulin gel, inulin gel/OVA, inulin/OVA, inulin (DP7)/OVA or inulin gel (DP10)/OVA for 20 days as specified in the schematic (OVA, 1 mg per dose; inulin, 55 mg per dose). The body weight of mice during OIT was recorded. All the mice received oral OVA challenges starting day 49. In guanosine/OVA OIT studies, OVA-sensitized mice were orally administered with inulin gel/OVA or free OVA and fed with normal drinking water as controls. In the OVA/guanosine group, OVA-sensitized mice were orally administered with free OVA and fed with drinking water containing 37.5 μg ml^{-1} guanosine. In the escalation/maintenance-dosing setting, sensitized mice were orally administered with OVA or inulin gel/OVA using 0.25, 0.5, 1, 2, 4, 8, 12 and 16 mg heated OVA (heating at 70 °C for 2 min), followed by 20 mg of heated OVA for six times. The mice were deprived of food for 4–6 h and intragastric challenged with 50 mg OVA in 250 μl PBS on six alternating days in 2 weeks. The body weight was recorded, and the body temperature during the last time of intragastric challenge was measured by a rectal probe for mice (Kent Scientific). All the other mouse allergy models can be found in Supplementary Methods.

In vivo immunological analyses of the small intestinal tissue and MLN

Here, 24 h after the intragastric challenge, the MLN and small intestinal tissues (jejunal and ileal segments) were collected. MLN were processed and filtered through a 70 μm strainer and resuspended at 50 million cells per ml. One million MLN cells were stained with CD16/32 block antibody (clone 93, eBiosciences) for staining of transcription factors. The other part of the MLN cells were seeded in a 96-well plate (10^6 cells per well) in the presence of PMA and ionomycin (1:500 dilution, eBiosciences). Then, 2 h later, brefeldin A was added (BioLegend). The cells were obtained 2 h later for intracellular cytokine staining. For the small intestinal tissues, the tissues were cut into small pieces, repeatedly washed and then stirred with Hank's balanced salt solution containing 1 mM dithiothreitol, 2.5% foetal bovine serum and 1 mM ethylene diamine tetraacetic acid at 37 °C for 30 min. Tissues were then digested with collagenase (type 3, Worthington Biochemical), DNase I (0.1 mg ml^{-1}) and Hank's balanced salt solution with 2.5% foetal bovine serum for 60 min. Subsequently, cell suspensions were isolated with Percoll (Fisher Scientific) solution (40:75%). Cells in the middle layer were collected for further flow cytometry analysis. Cells were blocked with anti-CD16/32 and then stained with the designated antibodies: allophycocyanin (APC)-eFluor 780-CD45 rat anti-mouse (clone 30 F11, eBioscience), PerCP-Cy5.5-CD3e Armenian hamster anti-mouse (clone 145 2C11, eBioscience), phycoerythrin (PE)-Cy7-CD4 rat anti-mouse (clone GK1.5, eBioscience), APC-FOXP3 monoclonal antibody (clone FJK-16s, eBioscience), PE-IL-4 rat anti-mouse (clone 11B11, eBioscience), FITC-IL-10 rat anti-mouse (clone JES5-16E3, eBioscience), BV421-anti-mouse IFNγ (clone XMG1.2, BioLegend), PE-T-bet mouse anti-human mouse (clone 4B10, eBioscience), Alexa Fluor 488-GATA-3 rat anti-mouse (clone TWAJ, eBioscience), BV421-RORγt mouse anti-mouse (clone Q31-378, BD). The cells were analysed at the Flow Cytometry Core, University of Michigan, with a ZE5 cell analyser (BioRad) or Cytek Aurora analyser (Cytek Biosciences).

Antigen uptake in the small intestine

Alum/OVA-sensitized BALB/c mice received the OIT treatment and AIN-93M chow (alfalfa-free diet to avoid the noise signal, Fisher Scientific) was provided to mice for 3–4 days before tissue collection. Various samples including PBS, AF647-labelled OVA (Invitrogen), inulin/AF647-labelled OVA or inulin gel/AF647-labelled OVA (inulin, 55 mg per dose; AF647-labelled OVA, 200 μg per dose) were orally administered to mice. After 3 h, the mice were euthanized and the SI-LP cells (jejunal and ileal segments) were obtained as described in the 'In vivo immunological analyses of the small intestinal tissue and MLN' section. The cells were stained with fixable eFluor 450, PE-Cy7-CD11c Armenian hamster monoclonal antibody (clone N418, BioLegend), BV605 anti-mouse CX_3CR1 (clone SA011F11, BioLegend), PE-CD103 rat anti-mouse (clone M290, BD), FITC anti-mouse I-A/I-E (clone M5/114.15.2, BioLegend), BV711-F4/80 rat anti-mouse F4/80 (clone T45 2342, BD Biosciences). Cells were analysed by a ZE5 cell analyser.

scRNA-seq analysis of the small intestinal tissue

Twenty-four hours after the sixth intragastric challenge, small intestinal tissues (jejunal and ileal segments) were collected and processed as described in the 'In vivo immunological analyses of the small intestinal tissue and MLN' section. Cells were blocked with anti-CD16/32 antibody. Each group had three biologically independent samples, and these samples were stained with three anti-mouse Hashtag antibodies (TotalSeq-C0301, TotalSeq-C0302 and TotalSeq-C0303, BioLegend). After 30 min, Hashtag-labelled cells in each sample were counted and combined according to the group and cell-counting information. Cells in each group were purified so that the cell viability was at least over 70%. Single-cell RNA gene sequencing were conducted at the Advanced Genomics Core, University of Michigan. Cells were processed via 10× Genomics 5' scRNA single-cell assay and the depth was above 50,000 reads per cell.

Single-cell clustering was performed as we previously described[50]. In brief, we normalized the scRNA-seq data by using the Seurat sctransform pipeline to regress out the g2m.score, s.score and mitochondrial percentage. Then, we used a combination of 3,000 highly variable genes and a panel of anchor genes to stabilize the immune cell subtype architecture. This anchor panel contained the following genes: *Cxcr5*, *Cd86*, *Ifnb1*, *Cd274*, *Irf5*, *Irf3*, *Ly6e*, *Tnf*, *Itgax*, *Lag3*, *Isg15*, *Icos*, *Gsdmd*, *Cd40*, *Fcer1a*, *Cd80*, *Il10*, *Tgfb1*, *Batf2*, *Cxcl9*, *Mrc1*, *Bcl6*, *Siglec15*, *Cd79a*, *Trdc*, *Tnfrsf4*, *Cd2*, *Tigit*, *Trac*, *Cd4*, *Ctla4*, *Cd8b1*, *Mx1*, *Foxp3*, *Tmem173*, *Trbc1*, *Ifna4*, *Trbc2*, *Pdcd1*, *Gzmb*, *Cd69*, *Eomes*, *Cd3d*, *Lgals9*, *Cd3e*, *Ncr1*, *Il6*, *Cd19*, *Nos2*, *Cd79b*, *Itgam*, *Batf3*, *Aim2*, *Xcr1*, *Gata3*, *Rorc*, *Il17a*,

Havcr2, *Cxcl10*, *Il3ra*, *Ifng*, *Nrp1*, *Tbx21*, *Ifnl3*, *Irf1*, *Cd14*, *Ly6g*, *Ly6c1*, *Cd8a* and *Lyz2*. The annotation of each cell cluster was performed by using singleR and manual review of marker matrices as well as the most highly expressed genes that drove the cluster distinction. The cluster sizes among the conditions were compared using the R package ALDEx2. Normalized data were used to identify differentially expressed genes.

Microbial community analyses

Alum/OVA-sensitized BALB/c mice received OIT treatment as described in the 'In vivo sensitization, OIT and challenges' section. Faecal pellets were collected on day 48, whereas the ileal contents were collected on day 49. The microbiome DNA were isolated via a Qiagen MagAttract power microbiome kit by the University of Michigan's Microbiome Core; the DNA were further amplified, and the 16S rRNA gene-sequencing analysis was performed. Briefly, the V4 region of 16S rRNA-encoding gene was amplified from the extracted DNA via barcoded dual-index primers. The pooled amplicon library was then sequenced on the Illumina MiSeq platform using the 500-cycle MiSeq V2 reagent kit. The raw 16S rRNA gene-sequencing data were FASTQ files and analysed using mothur (v. 1.40.5) with Silva reference files (release 132, silva.nr_v132.align) to align the sequences[51]. After a series of commands to reduce the sequencing and PCR errors, de-noise sequences and remove chimaeric sequences, the sequences were classified via a Bayesian classifier, using silva.nr_v132.align and silva.nr_v132.tax as the reference and taxonomy, respectively[20].

Untargeted metabolomics analyses

Alum/OVA-sensitized BALB/c mice received OIT treatment as described in the 'In vivo sensitization, OIT and challenges' section. Faecal pellets were collected on day 48, whereas the ileal contents were collected on day 49. The samples were stored in a −80 °C freezer until the day of metabolite extraction. On the day of extraction, the samples were transferred to bead-filled homogenization tubes and 300 µl of chilled 50% methanol solution was added followed by 10 µl of internal standard mixture of QReSS[52]. Samples were then homogenized using Precellys + Cryolys Evolution homogenizer at the following settings: 4 °C, 6,000 r.p.m., 4 × 20 s cycle, 120 s pause time. An additional 300 µl of chilled 50% methanol solution was added, vortexed and transferred to a fresh tube. Then, 600 µl of chloroform was added, vortexed for 15 min and followed by centrifugation at 1,700*g* at 4 °C for 15 min. The polar supernatants were dried and stored in the −80 °C freezer until ready for further processing. The dried samples were reconstituted in 50% methanol solution (150 µl) and then passed through 0.2 µm micro-centrifuge filter tube. Thereafter, 50 µl of filtrates from each sample were pooled and used for method development and quality control, whereas 100 µl of filtrates were transferred to LC vials (with 100 µl inserts) for analysis using the sample-specific optimized method. Filtrates were detected with SCIEX Triple Quad 7500 LC-MS/MS- QTRAP system coupled with an ExionLC system. The optimized-schedule multiple reaction monitoring (MRM) mass spectrometry method ran concurrently in both positive and negative ionization modes based on our in-house multiple reaction monitoring list of over 800 metabolites. The mass spectrometry method was set up as reported previously[53]. Peaks were extracted using SCIEX OS (v. 2.1.6.59781) and our in-house algorithm, implemented in R (CRAN 4.1.1), was utilized to filter out the analytes with poor quality. Only unique metabolites with good quality across all the samples were considered in the downstream analysis. Peaks were further normalized to the internal standards, and metabolite abundance was normalized to the weight of faecal/ileal matter. Further downstream analyses were performed in Metaboanalyst (v. 5.0)[54] and GraphPad Prism (8.0).

Association study between ileal metabolomics and microbial data via machine learning

Paired metabolomics (dataset X) and microbial data (dataset Y) obtained from ileal contents from 36 samples (five naive, eight PBS, seven OVA, eight inulin/OVA and eight inulin gel/OVA samples) were utilized in the association study. The association study was based on the 'HAIIA' (v. 0.8.20) testing algorithm[44]. In brief, Spearman's correlation was used to separately compute the similarity (distance) score within datasets X and Y. This step separately generated hierarchical clusters of both metabolites and microbial family (or genus) that were similar to each other and arranged in the order of similarity. Next, HAIIA learned the significance of pairwise association between each and every cluster from datasets X and Y using Benjani–Hochberg false discovery rate. If a paired association was not significant, HAIIA iteratively performed the act of separately dropping branches from both clusters and the act that yielded a better Gini impurity score was retained. The iteration continued until a statistically significant block of association was achieved or until the block of association was reduced to only a pair of features from both datasets, whichever came first. Blocks of association were arranged in the order of their significance and a heat map was generated. On this map, the solid numbers represent the rank of the block of associations. Number 1 indicates that the association represented in block 1 is the most statistically significant block, followed by block 2 and so on. Only features that show up in any of the significant clusters were shown on the heat map (HAllAgram). The heat map also displayed the Spearman's pairwise correlation score between features from datasets X and Y. For the current analysis, a false discovery rate threshold of 0.5 was used for the block associations to visualize all the potentially important associations between the clusters of microbial and metabolomics features.

Mast cell quantification in the small intestine

Here, 24 h after the last intragastric challenge of OVA, jejunal tissue was collected and fixed in 4% formalin. The tissues were stained with toluidine blue via the In-Vivo Animal Core, University of Michigan. At least three random sections per mouse were analysed, and toluidine blue-positive stained cells were counted from around 5 mm length of tissue (magnification, ×20).

Small intestinal retention imaging

To prepare FITC-labelled inulin gel/Texas Red-labelled OVA, 53.5 mg inulin and 1.5 mg FITC-labelled inulin (Sigma-Aldrich) were mixed in 150 µl PBS buffer, followed by inulin gel formation, as described in the 'Preparation and characterization of inulin gel/allergen formulations' section. After cooling down, FITC-labelled inulin gel, 0.1 mg Texas Red-labelled OVA (Invitrogen) and 0.9 mg native OVA were mixed to get FITC-labelled inulin gel/Texas Red-labelled OVA. Alum/OVA-sensitized BALB/c mice (female, 5–6 weeks old, from Jackson Laboratory) were fed with AIN-93M chow for 3–4 days and then the mice were gavaged with 150 µl FITC-labelled inulin gel/Texas Red-labelled OVA. The mice were deprived of chow post-oral gavage and euthanized at 100, 200 and 300 min. The small intestine was harvested and imaged via the IVIS optical imaging system, using an FITC channel to observe inulin or the Texas Red channel to observe OVA.

Small intestinal barrier integrity

Alum/OVA-sensitized BALB/c mice received OIT treatment, repeated intragastric challenges as described in the 'In vivo sensitization, OIT and challenges' section. On day 57, the mice were fasting for 4 h, followed with the oral administration of FITC-dextran (Sigma-Aldrich, 10 mg per dose) in 150 µl PBS buffer. The serum samples were collected 3 h post-oral gavage and the fluorescence intensity of FITC was detected via a microplate reader.

Statistical analysis

The results are expressed as the mean ± s.e.m. A one-way or two-way ANOVA, followed by Bonferroni's multiple comparisons test, analysis of molecular variance or two-sided, unpaired Student's *t*-test or Mann–Whitney test was used for testing the differences between

groups. All the animal studies were performed after randomization. Data collection and analysis were not performed blind to the conditions of the experiments. No statistical methods were used to pre-determine the sample sizes but our sample sizes are similar to those reported in previous publications[8,21]. Data were approximately normally distributed and the variance was similar between the groups. The experiments were repeated multiple times as independent experiments, as indicated in the figure captions. A complete dataset from one representative, independent experiment is shown in the figures. No samples were excluded from the analyses. GraphPad Prism 8.0 software was used for the statistical analyses.

Reporting summary

Further information on research design is available in the Nature Portfolio Reporting Summary linked to this article.

Data availability

The scRNA data have been deposited in the NCBI Sequence Read Archive (accession no. PRJNA1074271). The bacterial 16S rRNA-sequencing data have been deposited in the NCBI Sequence Read Archive (accession no. PRJNA1073670). The data supporting the findings of this study are available within the Article and its Supplementary Information files. All relevant data are available from the corresponding author. Source data are provided with this paper.

References

49. Barletta, B. et al. Probiotic VSL# 3-induced TGF-β ameliorates food allergy inflammation in a mouse model of peanut sensitization through the induction of regulatory T cells in the gut mucosa. *Mol. Nutr. Food Res.* **57**, 2233–2244 (2013).
50. Gong, W. et al. Cancer-specific type-I interferon receptor signaling promotes cancer stemness and effector CD8+ T-cell exhaustion. *Oncoimmunology* **10**, 1997385 (2021).
51. Kozich, J. J., Westcott, S. L., Baxter, N. T., Highlander, S. K. & Schloss, P. D. Development of a dual-index sequencing strategy and curation pipeline for analyzing amplicon sequence data on the MiSeq Illumina sequencing platform. *Appl. Environ. Microbiol.* **79**, 5112–5120 (2013).
52. Percy, A. J., Proos, R., Demianova, Z., Backiel, K. & Ubhi, B. K. Standardizing Quantitative Metabolomics Analyses Through the QReSS™ Kit.
53. Marvar, J. et al. Porous PDMS-based microsystem (ExoSponge) for rapid cost-effective tumor extracellular vesicle isolation and mass spectrometry-based metabolic biomarker screening. *Adv. Mater. Technol.* **8**, 2201937 (2023).
54. Pang, Z. et al. Using MetaboAnalyst 5.0 for LC–HRMS spectra processing, multi-omics integration and covariate adjustment of global metabolomics data. *Nat. Protoc.* **17**, 1735–1761 (2022).

Acknowledgements

This work was supported by the National Institutes of Health (NIH) (R01DK125087, R01DE030691, R01DE026728, R01DE031951, R01NS122536, R01CA210273, R01CA271799, R01CA271369, R01CA227622, R01CA222251, R01CA204969 and P30CA046592 to J.J.M. and U01DE033330 to Y.L.L.). Y. Xie is supported by NIH funding R01HL166508 and an NSF award IOS 2107215. D.N. is supported by a Rogel Cancer Center grant and a Forbes Scholar Award. We thank the NIH Tetramer Core Facility (contract HHSN272201300006C) for provision of MHC-I tetramers.

Author contributions

K.H., F.X. and J.J.M. designed the study. K.H. and F.X. performed the experiments. O.A., M.N., F.W., K.O., A.A., S.C. and D.N. assisted with the measurement and analysis of short-chain fatty acids and untargeted metabolomics. O.A. performed the machine learning analysis. J.J.O. assisted with the casein and peanut allergy model studies and provided useful discussion. S.K., Y.K. and N.K. assisted with the small intestine studies. M.T.P., Y.S.C., H.D. and Q.W. provided technical help with immune cell analyses in the colon and lungs. J.X., X.Z., X.H., J.A., M.T.P., X.A., Y. Xu and S.-H.L. provided technical help with flow cytometry, NMR and MALDI-TOF. A.K. assisted in the rheology test. Z.L., W.G., Y. Xie and Y.L.L. assisted with the scRNA-seq experiments and analysis. K.H., F.X. and J.J.M. interpreted the data and wrote the paper.

Competing interests

Patent applications for inulin-gel-based treatment for allergies and other disorders have been filed in the USA, Europe, Japan, South Korea, China, Australia and Canada (US20230346826, WO2022066825, US20220347294 and WO2021061789), with J.J.M., K.H., F.X., J.X., X.H. and X.Z. as inventors. J.J.M. declares financial interests for board membership, as a paid consultant, for research funding, and/or as an equity holder in EVOQ Therapeutics and Saros Therapeutics. The University of Michigan has a financial interest in EVOQ Therapeutics, Inc. The other authors declare no competing interests.

Additional information

Extended data is available for this paper at https://doi.org/10.1038/s41563-024-01909-w.

Supplementary information The online version contains supplementary material available at https://doi.org/10.1038/s41563-024-01909-w.

Correspondence and requests for materials should be addressed to James J. Moon.

Peer review information *Nature Materials* thanks Nicola Harris, Tian Xia and the other, anonymous, reviewer(s) for their contribution to the peer review of this work.

https://doi.org/10.1038/s41563-024-01909-w

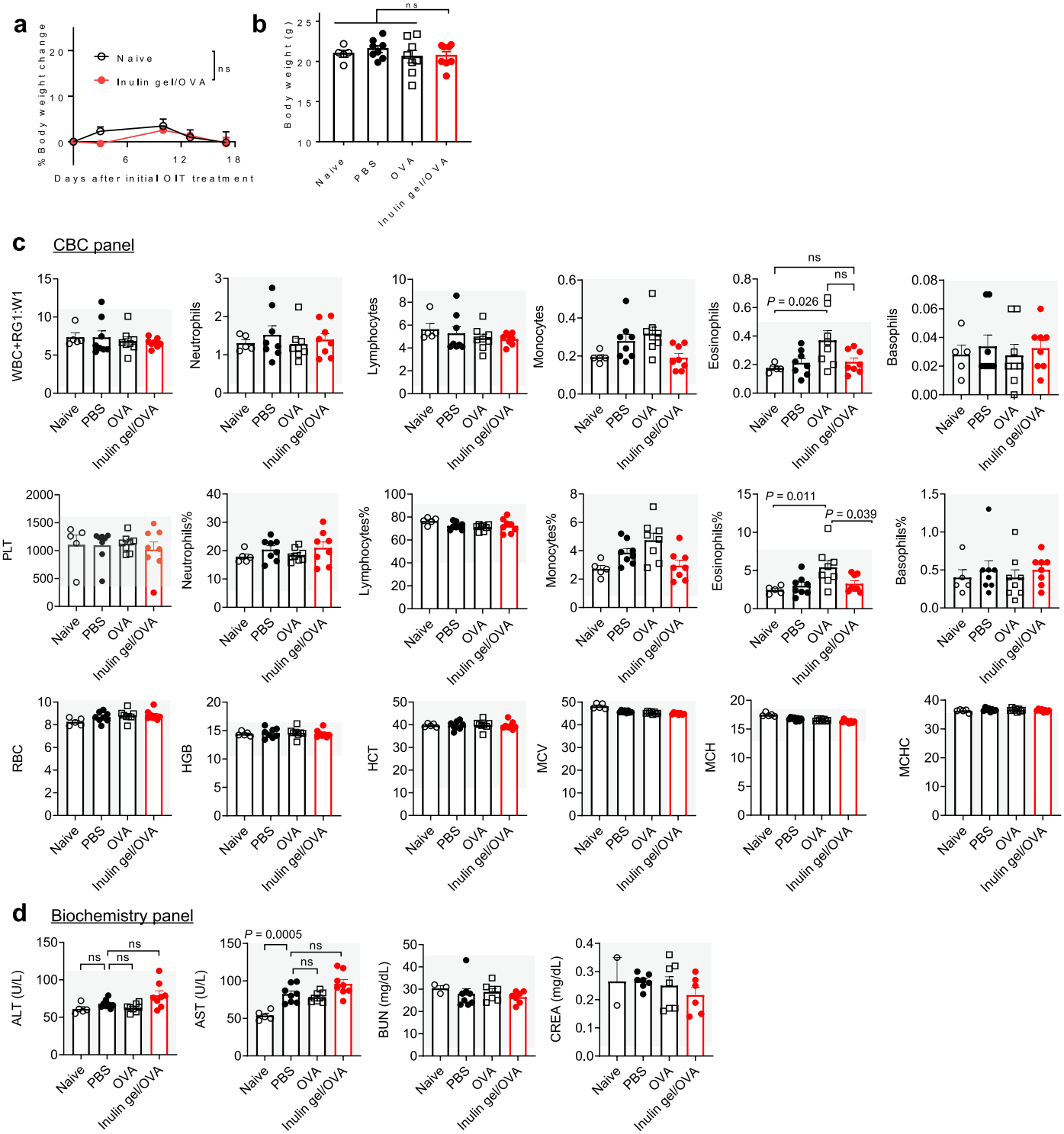

Extended Data Fig. 1 | Biosafety evaluation. BALB/c mice were treated as in Fig. 1b. The bodyweight changes during OIT (**a**) and body weight on day 48 (**b**) were recorded. (**c**) Blood samples were collected for CBC test on day 48. (**d**) Serum samples were collected for biochemistry test on day 48. Data represent mean ± s.e.m. (n = 5 for Naive, 7 for Inulin gel/OVA (**a**), n = 5 for Naive, 8 for all other groups (**b,c**), n = 5 for Naive, 8 for all other groups in ALT and AST datasets, 3 for Naive, 8 for PBS or 7 for all other groups in BUN dataset, 2 for Naive, 8 for PBS and OVA, or 6 for Inulin gel/OVA in CREA dataset (**d**) biologically independent samples). ns: not significant. Data were analysed by one-way (**b-d**) or two-way ANOVA (**a**) with Bonferroni's multiple comparisons test.

https://doi.org/10.1038/s41563-024-01909-w

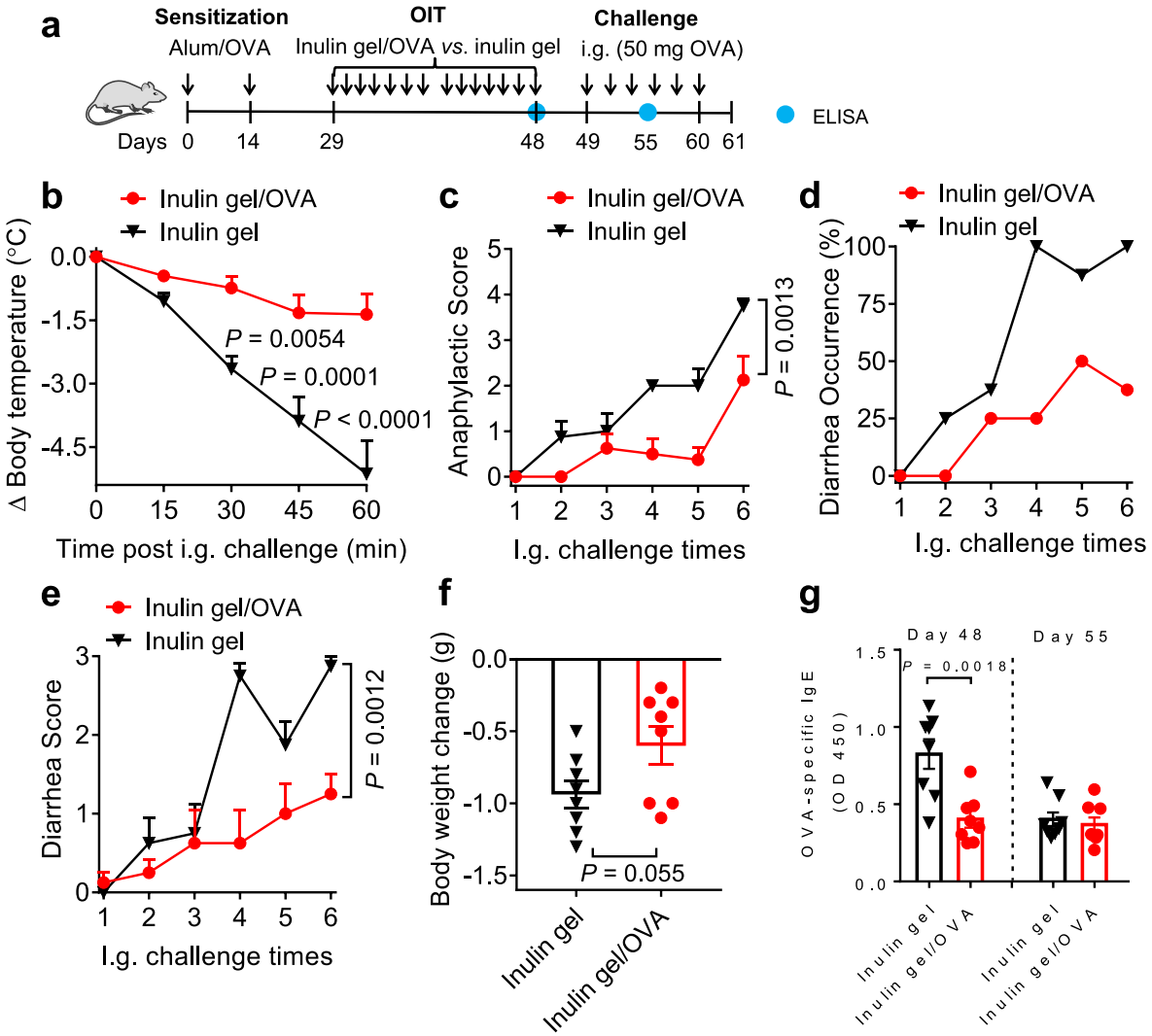

Extended Data Fig. 2 | Inulin gel/OVA OIT protects against OVA challenges. **a**, Therapeutic regimen. BALB/c mice were sensitized with alum/OVA on days 0 and 14. From day 29, the mice were orally gavaged with inulin gel (55 mg per dose), or inulin gel (55 mg per dose)/OVA (1 mg per dose). From day 49, mice were intragastrically (i.g.) challenged with OVA (50 mg per dose) on 6 alternating days. Shown are the (**b**) average body temperature change after the 6th challenge, (**c**) anaphylactic scores, (**d**) diarrhea occurrence rate, and (**e**) diarrhea severity during challenges. **f**, Diarrhea-induced body weight change after the 6th i.g. challenge. **g**, OVA-specific IgE levels in serum on days 48 and 55. Data represent mean ± s.e.m. (n = 8 biologically independent samples). Data were analysed by two-way ANOVA (**b**,**c**,**e**) with Bonferroni's multiple comparisons test, or unpaired, two-sided Student's t-test (**f**,**g**).

https://doi.org/10.1038/s41563-024-01909-w

a

Vendor	DP via ^{1}HNMR	Mw from MALDI-TOF
Sigma-Aldrich	23	~3906
Now Foods	10	~1800
Swanson	7	~1314

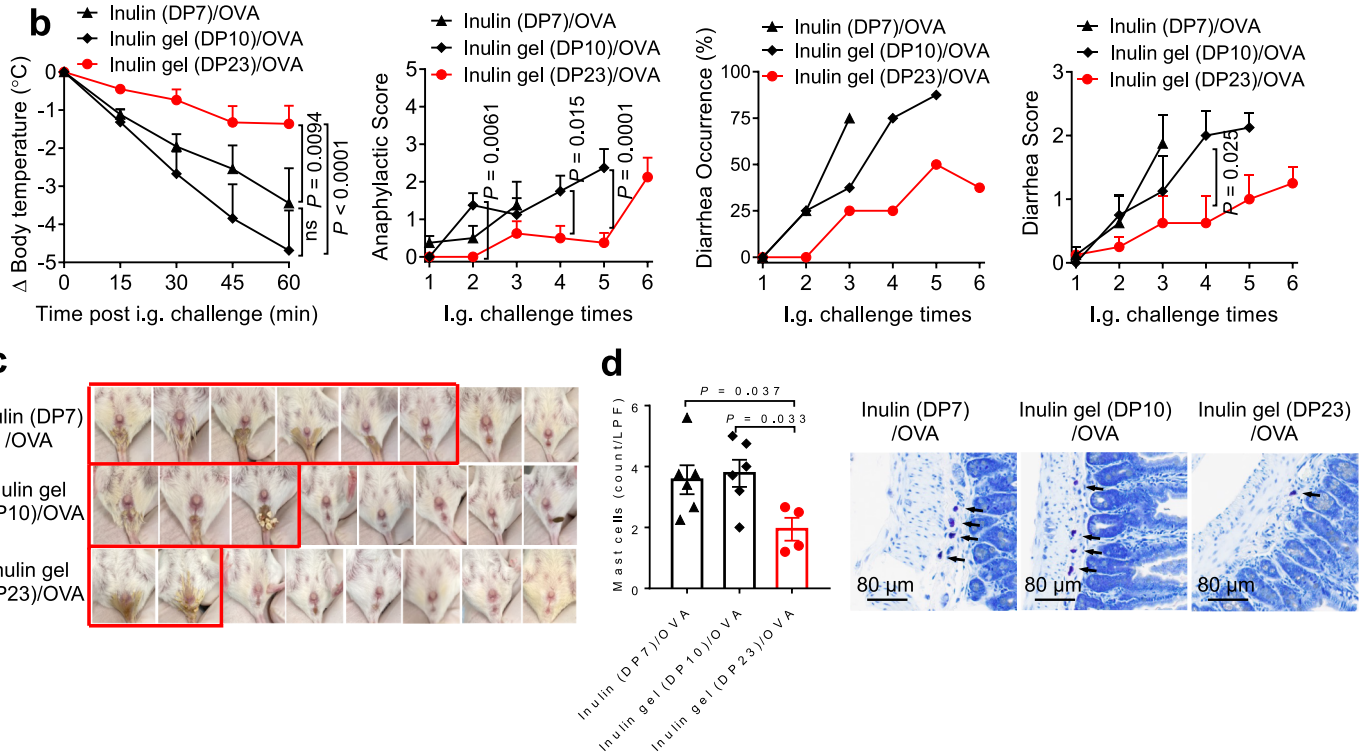

Extended Data Fig. 3 | DP values of inulin affect OIT efficacy. a, The DP values of inulin from different vendors were measured by ^{1}HNMR and MALDI-TOF. **b**, BALB/c mice were treated as in Fig. 1b and received OIT treatments of inulin (DP7)/OVA, inulin gel (DP10)/OVA, and inulin gel (DP23)/OVA, respectively. Mice were i.g. challenged for 6 times. The body temperatures during the 6th i.g. challenge, the anaphylactic symptoms, diarrhea occurrence rate and severity during the challenges were recorded. **c**, The diarrhea images at the 3rd i.g. challenge. **d**, Average mast cells and the representative images in ileum. Data represent mean ± s.e.m. (In body temperature, n = 7 for Inulin (DP7)/OVA and Inulin gel (DP10)/OVA, or 8 for Inulin gel (DP23)/OVA, in all other datasets, n = 8 (**b**), n = 6 for Inulin (DP7)/OVA, Inulin gel (DP10)/OVA, 4 for Inulin gel (DP23)/OVA (**d**) biologically independent samples). ns, not significant. Data were analysed using two-way ANOVA (**b**), or one-way ANOVA (**d**) with Bonferroni's multiple comparisons test.

https://doi.org/10.1038/s41563-024-01909-w

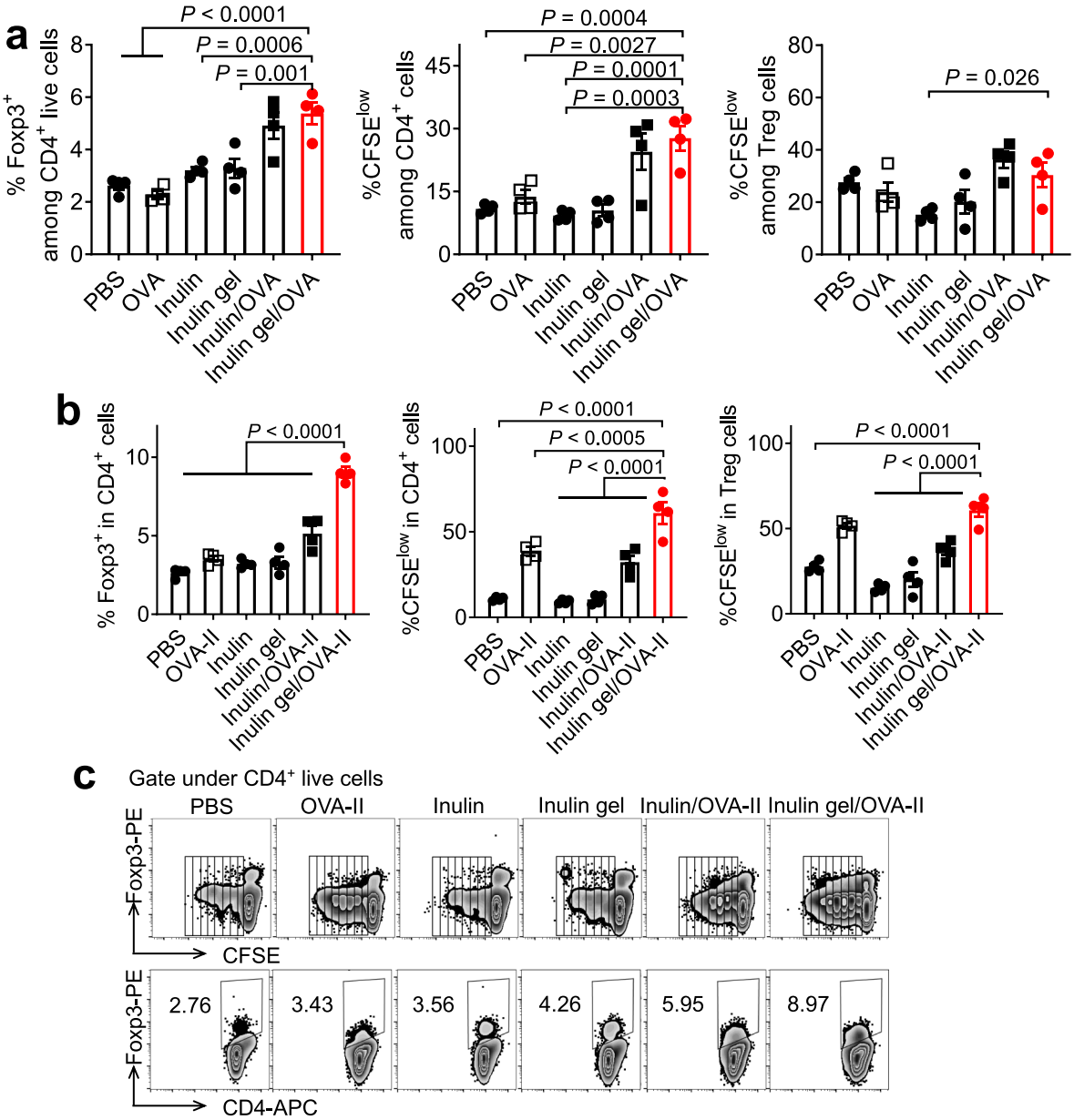

Extended Data Fig. 4 | In vitro Treg cell differentiation. BMDCs were treated with inulin gel/OVA or inulin gel/OVA-II peptide for 24 h. BMDCs were washed and co-cultured with CFSE-labeled OT-II $CD4^+$ T cells. Shown are the frequency of $Foxp3^+CD4^+$ T cells, proliferating $CFSE^{low}$ cells, and representative flow cytometry plots after 5 days of co-culture. Data represent mean ± s.e.m. (n = 4 biologically independent samples). Data were analysed by one-way ANOVA with Bonferroni's multiple comparisons test.

https://doi.org/10.1038/s41563-024-01909-w

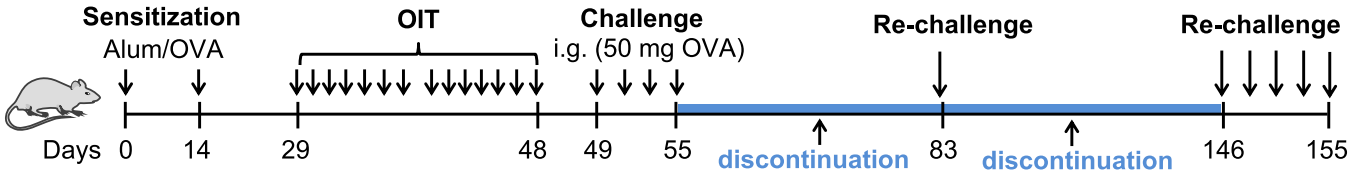

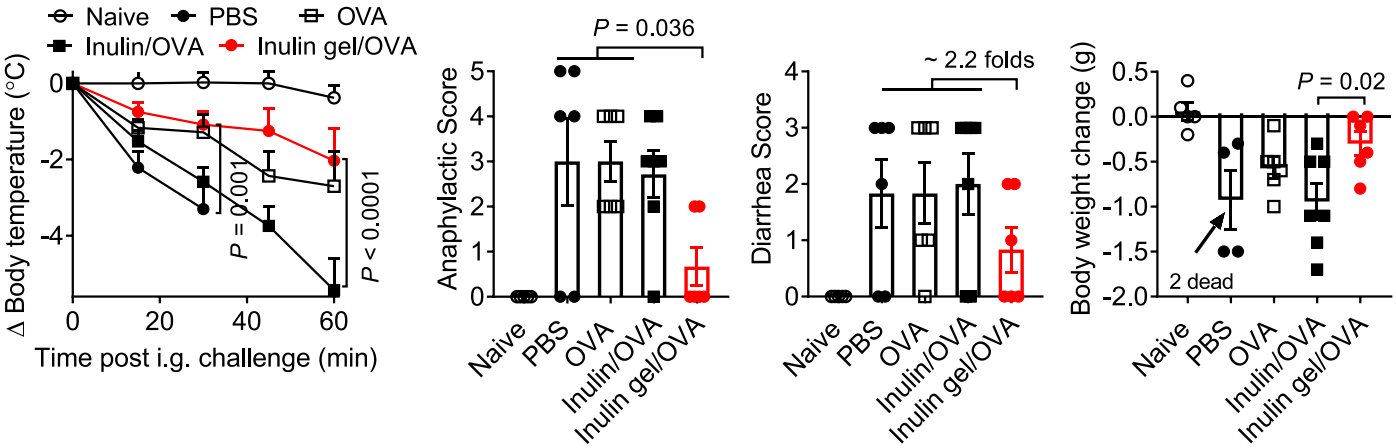

Extended Data Fig. 5 | Long-term protection. Alum/OVA-sensitized mice received the indicated OIT treatment, followed by 4 times of i.g. challenges of OVA protein. The doses of inulin and OVA were 55 mg and 1 mg, respectively. All treatments were discontinued from day 55. From day 146, the mice were i.g. challenged with OVA. Shown are the body temperature drop, anaphylactic score, diarrhea score, and body weight change during the 5th i.g. re-challenge. Data represent mean ± s.e.m. (n = 5 for Naive, 7 for Inulin/OVA or 6 for all other groups, biologically independent samples). Data were analysed by one-way or two-way ANOVA with Bonferroni's multiple comparisons test.

https://doi.org/10.1038/s41563-024-01909-w

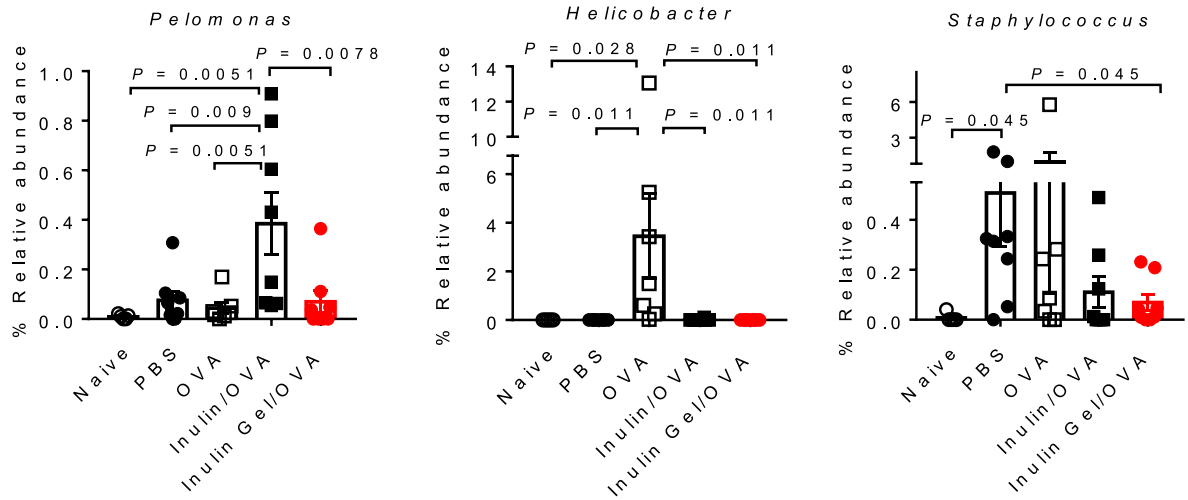

Extended Data Fig. 6 | Microbes abundances in ileal contents. Alum/OVA-sensitized BALB/c mice were treated as in Fig. 1b. Shown are the relative abundances of several genera in the ileal contents. Data represent mean ± s.e.m. (n = 5 for Naive, 7 for OVA or 8 for all other groups, biologically independent samples). Data were analysed by one-way ANOVA with Bonferroni's multiple comparisons test.

https://doi.org/10.1038/s41563-024-01909-w

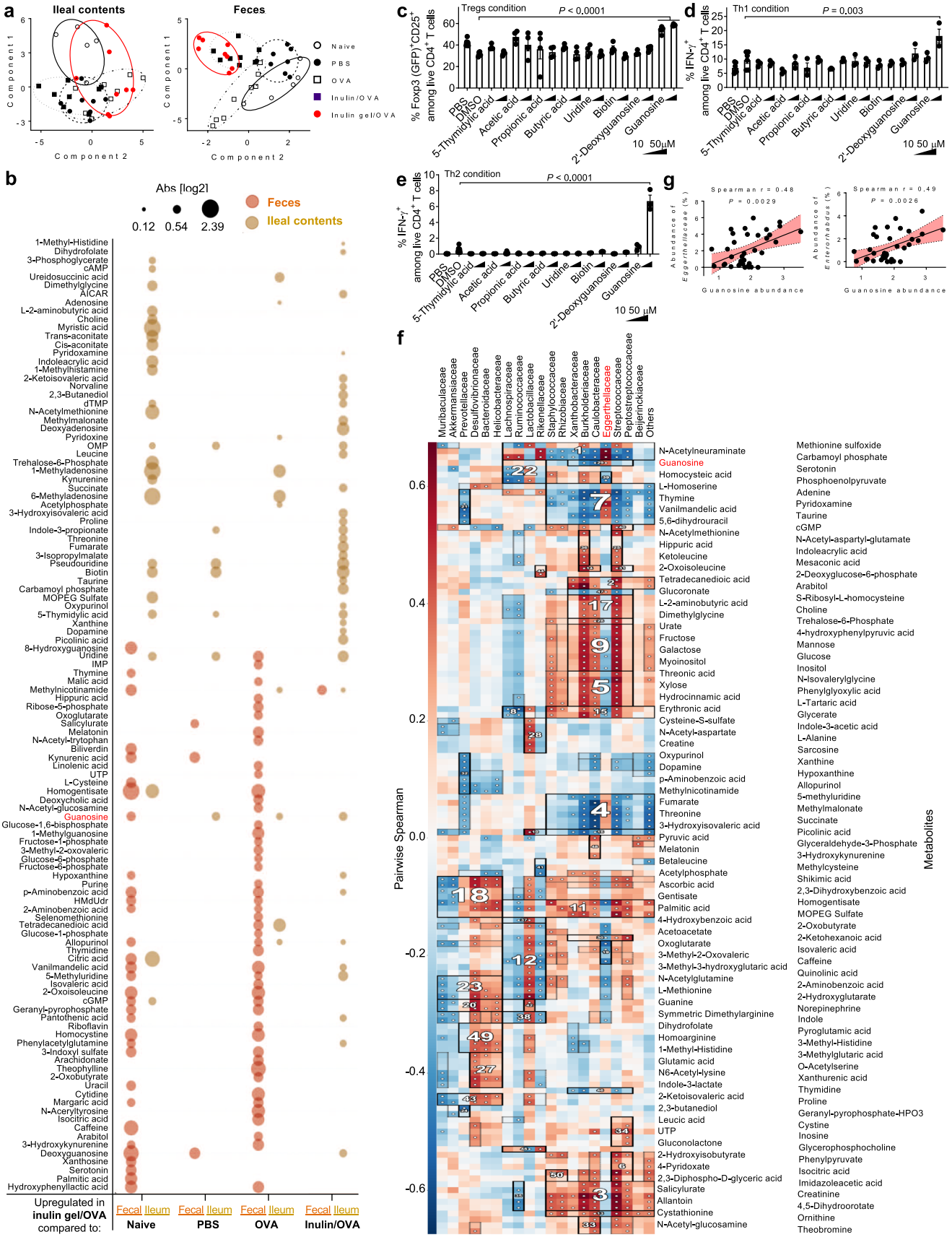

Extended Data Fig. 7 | See next page for caption.

https://doi.org/10.1038/s41563-024-01909-w

Extended Data Fig. 7 | Immunomodulatory guanosine as identified by metabolomics and machine learning based analyses. Alum/OVA-sensitized BALB/c mice were treated as in Fig. 1b. **a-b**, Untargeted metabolome analysis in the ileal contents and feces. Shown are the sPL-SDA analysis of the metabolites in the ileal contents on day 49 and feces on day 48 (**a**), fold changes of metabolites (whose *P*-value is less than 0.05) in the ileal and fecal contents. The size of the circle denotes the fold change of upregulated metabolites in the inulin gel/OVA group, compared with naïve, PBS, OVA, and inulin/OVA groups. The *P*-values are unadjusted and are based on a two-sided t-test statistics (**b**). **c-e**, Metabolite-induced differentiation of $CD4^+$ T cells *in vitro*. $CD4^+$ T cells isolated from Foxp3(GFP) reporter mice were cultured with various metabolites in suboptimal Treg-inducing condition (1 μg/mL anti-CD3 antibody, 1 μg/mL anti-CD28 antibody, 5 ng/mL IL-2, and 1 ng/mL TGF-β) and analyzed on day 3 for Foxp3 expression (**c**). $CD4^+$ T cells isolated from wide-type (WT) C57BL/6 mice were cultured with various metabolites in T_H1-inducing condition (1 μg/mL anti-CD3 antibody, 1 μg/mL anti-CD28 antibody, 5 ng/mL IL-2, 10 ng/mL IL-12p40, and 10 μg/mL anti-IL-4 antibody) and analyzed on day 5 for IFN-γ secretion (**d**). $CD4^+$ T cells isolated from WT C57BL/6 mice were cultured with various metabolites in T_H2-inducing condition (1 μg/mL anti-CD3 antibody, 1 μg/mL anti-CD28 antibody, 5 ng/mL IL-2, 10 ng/mL IL-4, and 10 μg/mL anti-IFN-γ antibody) and analyzed on day 5 for IFN-γ secretion (**e**). **f**, Machine learning-based association study between ileal metabolomics and microbes at the family level. Only features with significant clusters were shown on the heatmap (Hallagram). **g**, Spearman's correlation coefficient analyses between the relative abundances of ileal guanosine and *Eggerthellaceae* (family) or *Enterorhabdus* (genus). Data represent the mean ± s.e.m. from one of two independent experiments (n = 5 for Naive or 8 for all other groups (**a**), n = 6 for PBS and DMSO, or 4 for all other groups (**c**), n = 6 for PBS and DMSO, or 3 for all other groups (**d,e**) biologically independent samples). Data were analysed by one-way ANOVA with Bonferroni's multiple comparisons test (**c-e**), or two-tailed Spearman's rank correlation test (**g**).

https://doi.org/10.1038/s41563-024-01909-w

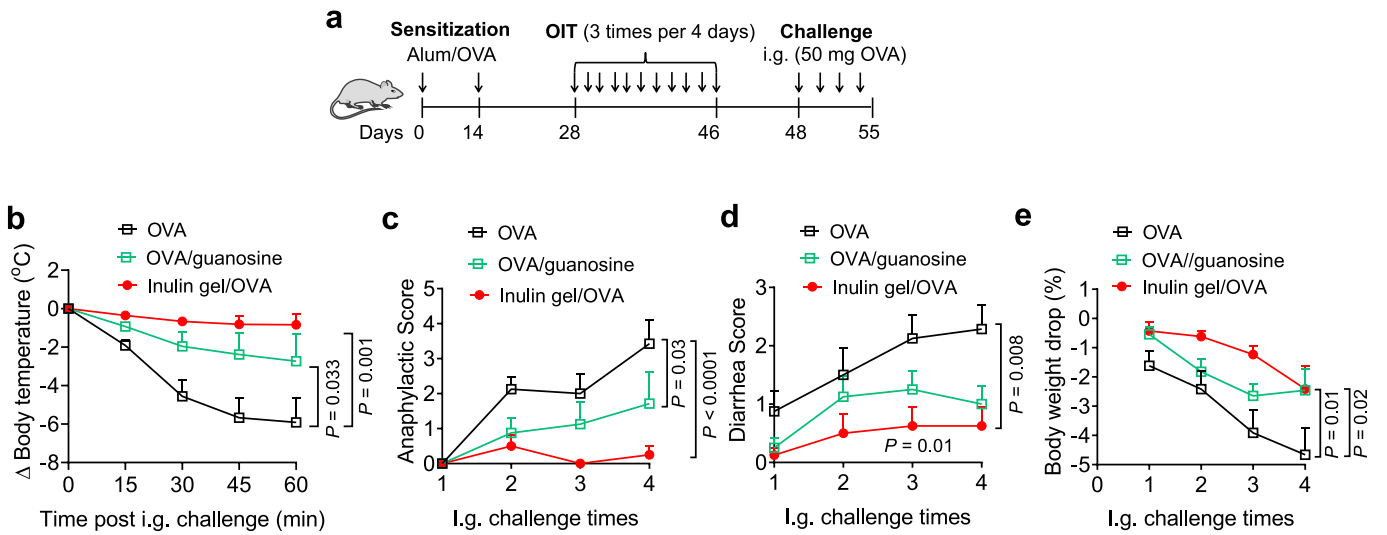

Extended Data Fig. 8 | OVA/guanosine OIT protects mice against allergen challenges. a, Schema of the intestinal anaphylaxis and therapeutic regimen of OVA/guanosine OIT. BALB/c mice were sensitized with alum/OVA on days 0 and 14. From day 28, mice were orally gavaged with OVA (1 mg per dose) and provided with normal drinking water either with or without 37.5 μg/mL of guanosine (denoted OVA and OVA/guanosine, respectively). Inulin gel (55 mg per dose)/OVA (1 mg per dose) treated mice that were provided with normal drinking water were included as an additional control. From day 48, mice were i.g. challenged with OVA (50 mg per dose) on 4 alternating days. **b**, After the 4th i.g. challenge, changes in core body temperature were measured. **c**-**e**, Over the 4 consecutive i.g. challenges, animals were analyzed for anaphylactic scores (**c**), diarrhea severity score (**d**), and body weight change (**e**). Data represent the mean ± s.e.m. (n = 8 for Inulin gel/OVA or 7 for all other groups (**b**), n = 8 (**c**-**e**) biologically independent samples). Data were analysed by two-way ANOVA with Bonferroni's multiple comparisons test.

https://doi.org/10.1038/s41563-024-01909-w

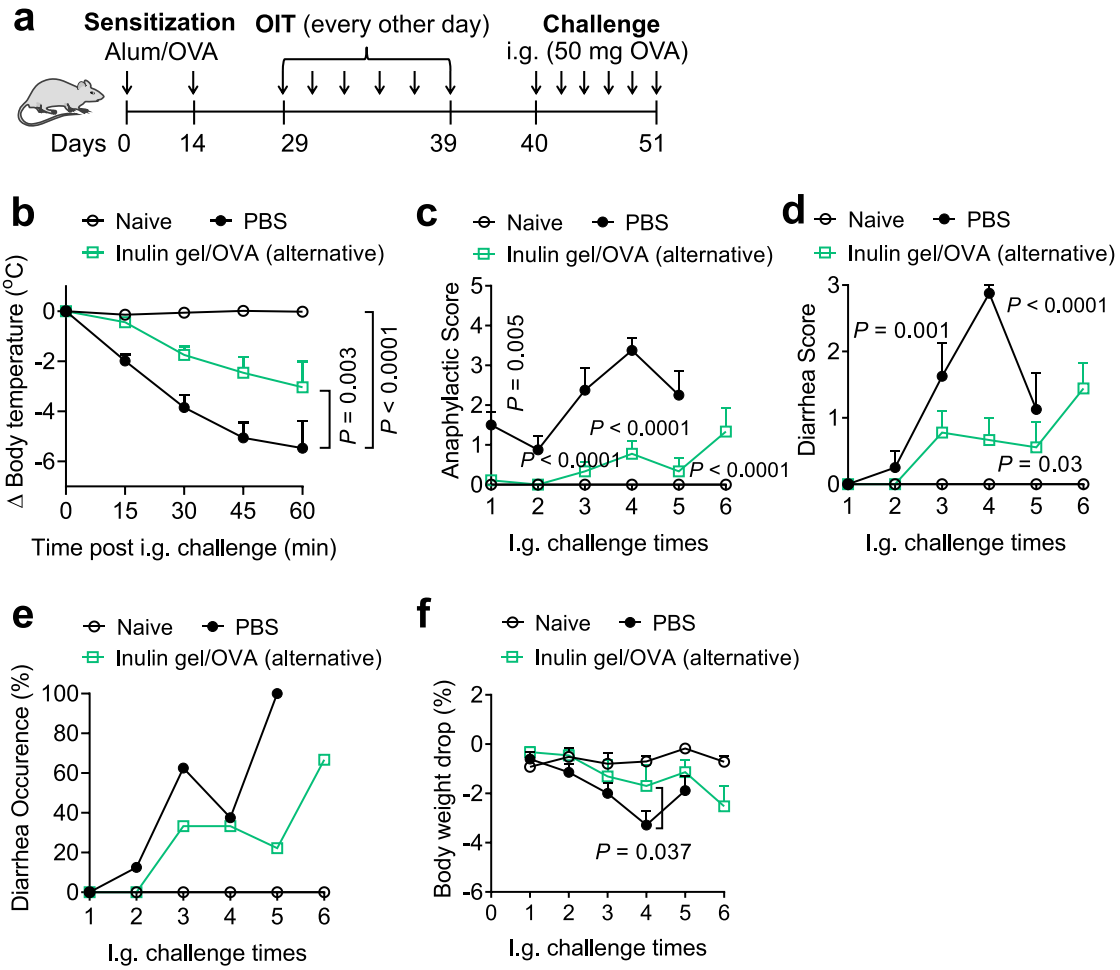

Extended Data Fig. 9 | Less frequent inulin gel/OVA OIT remains protective. Schema of the intestinal anaphylaxis and therapeutic regimen. BALB/c mice were sensitized with alum/OVA on days 0 and 14. From day 29, mice were orally gavaged with PBS, OVA (1 mg per dose), or inulin gel (55 mg per dose)/OVA (1 mg per dose) every other day. From day 40, mice were i.g. challenged with OVA (50 mg per dose) on 6 alternating days. **b**, After the 6th i.g. challenge, changes in the average core body temperature were measured. **c-f**, Over the 6 consecutive i.g. challenges, animals were analyzed for anaphylactic scores (**c**), diarrhea severity score (**d**), diarrhea occurrence rate (**e**), and bodyweight drop (**f**). Data represent mean ± s.e.m. (n = 5 for Naive, 8 for PBS or 9 for Inulin gel/OVA (alternative) (**b-f**) biologically independent samples). Data were analysed by two-way ANOVA (**b-d**,**f**) with Bonferroni's multiple comparisons test.

https://doi.org/10.1038/s41563-024-01909-w

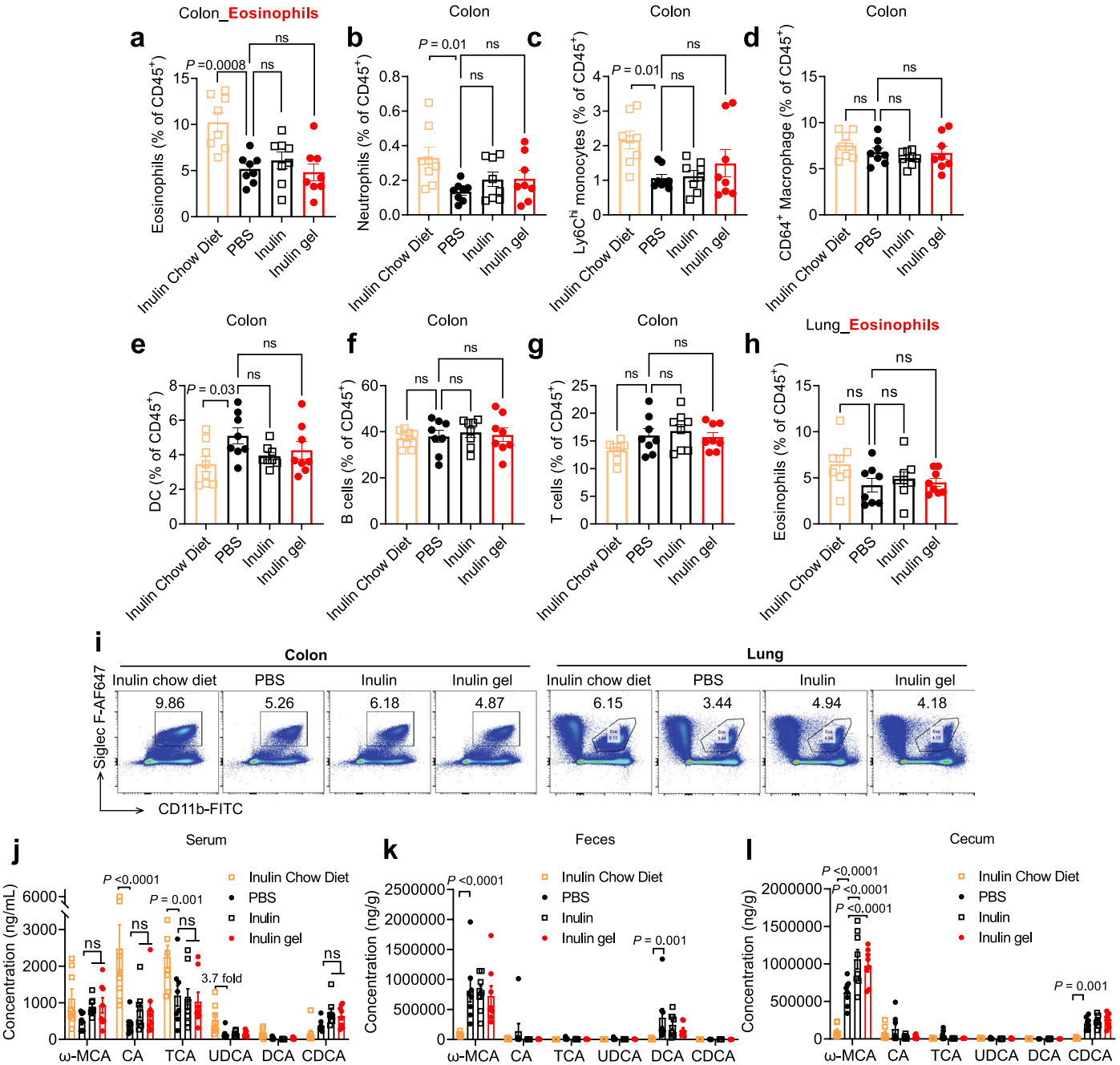

Extended Data Fig. 10 | Inulin gel does not induce type 2 inflammatory response. Naive C57BL/6 mice were fed with high (26%) inulin chow diet, control chow diet (0% inulin, PBS group), control chow diet plus inulin (55 mg/dose, 3 times per 4 days, inulin group), or control chow diet plus inulin gel (55 mg/dose, 3 times per 4 days, inulin gel group). On day 13, the frequencies of immune cells in the colon were detected: (**a**) eosinophils; (**b**) neutrophils; (**c**) Ly6C^{high} monocytes; (**d**) CD64^{+} macrophages; (**e**) DCs; (**f**) B cells; (**g**) T cells. (**h**) The frequency of eosinophils in the lung. (**i**) The representative flow plot of eosinophils in the colon and lung. The concentrations of ω-MCA, CA, TCA, UDCA, DCA, and CDCA in the (**j**) serum, (**k**) feces, and (**l**) cecum on day 13. Data represent mean ± s.e.m. (n = 8 biologically independent samples). ns: not significant. Data were analysed by (**a-h**) one-way, or (**j-l**) two-way ANOVA with Bonferroni's multiple comparisons test.

nature portfolio

Corresponding author(s): James J. Moon

Last updated by author(s): Mar 10, 2024

Reporting Summary

Nature Portfolio wishes to improve the reproducibility of the work that we publish. This form provides structure for consistency and transparency in reporting. For further information on Nature Portfolio policies, see our Editorial Policies and the Editorial Policy Checklist.

Statistics

For all statistical analyses, confirm that the following items are present in the figure legend, table legend, main text, or Methods section.

n/a	Confirmed	
☐	☒	The exact sample size (*n*) for each experimental group/condition, given as a discrete number and unit of measurement
☐	☒	A statement on whether measurements were taken from distinct samples or whether the same sample was measured repeatedly
☐	☒	The statistical test(s) used AND whether they are one- or two-sided *Only common tests should be described solely by name; describe more complex techniques in the Methods section.*
☐	☒	A description of all covariates tested
☐	☒	A description of any assumptions or corrections, such as tests of normality and adjustment for multiple comparisons
☐	☒	A full description of the statistical parameters including central tendency (e.g. means) or other basic estimates (e.g. regression coefficient) AND variation (e.g. standard deviation) or associated estimates of uncertainty (e.g. confidence intervals)
☐	☒	For null hypothesis testing, the test statistic (e.g. *F*, *t*, *r*) with confidence intervals, effect sizes, degrees of freedom and *P* value noted *Give P values as exact values whenever suitable.*
☒	☐	For Bayesian analysis, information on the choice of priors and Markov chain Monte Carlo settings
☐	☒	For hierarchical and complex designs, identification of the appropriate level for tests and full reporting of outcomes
☐	☒	Estimates of effect sizes (e.g. Cohen's *d*, Pearson's *r*), indicating how they were calculated

Our web collection on statistics for biologists contains articles on many of the points above.

Software and code

Policy information about availability of computer code

Data collection	Flow cytometric data were collected using a Ze5 cell analyzer (BD Biosciences) or a Cytek Aurora analyzer (Cytek Biosciences). Microbiome data from feces and ileal contents were collected using the MiSeq Illumina sequencing platform. In vivo images were acquired using IVIS Lumina Living Image Software(v.4.5.5). Metabolomics data were analyzed with SCIEX Triple QuadTM 7500 LC-MS/MS- QTRAP system coupled with ExionLCTM system. Single-cell RNA sequencing was conducted by the University of Michigan's Advanced Genomics Core.
Data analysis	Flow-cytometry analysis was done in BD FACSDiva and FlowJo (v.10.5) (Tree Star). Microbiome analysis was done in the community-supported software program mothur and by the steps in the MiSeq SOP (http://mothur.org/wiki/MiSeq_SOP). In vivo images were analysed using IVIS Lumina Living Image (v.4.5.5) Software. Metabolomics was analyzed using Metaboanalyst (V. 5.0). Statistical analysis was done in GraphPad Prism 8.0.

For manuscripts utilizing custom algorithms or software that are central to the research but not yet described in published literature, software must be made available to editors and reviewers. We strongly encourage code deposition in a community repository (e.g. GitHub). See the Nature Portfolio guidelines for submitting code & software for further information.

Data

Policy information about availability of data

All manuscripts must include a data availability statement. This statement should provide the following information, where applicable:

- Accession codes, unique identifiers, or web links for publicly available datasets
- A description of any restrictions on data availability
- For clinical datasets or third party data, please ensure that the statement adheres to our policy

The authors declare that data supporting the findings of this study are available within the article and its Supplementary Information files. All relevant data are available from the authors. The scRNA sequencing data have been deposited in the NCBI Sequence Read Archive (accession number: PRJNA1074271). The bacterial 16S rRNA sequencing data have been deposited in the NCBI Sequence Read Archive (accession number: PRJNA1073670).

Human research participants

Policy information about studies involving human research participants and Sex and Gender in Research.

Reporting on sex and gender	Not applicable
Population characteristics	Not applicable
Recruitment	Not applicable
Ethics oversight	Not applicable

Note that full information on the approval of the study protocol must also be provided in the manuscript.

Field-specific reporting

Please select the one below that is the best fit for your research. If you are not sure, read the appropriate sections before making your selection.

☒ Life sciences ☐ Behavioural & social sciences ☐ Ecological, evolutionary & environmental sciences

For a reference copy of the document with all sections, see nature.com/documents/nr-reporting-summary-flat.pdf

Life sciences study design

All studies must disclose on these points even when the disclosure is negative.

Sample size	No statistical methods were used to pre-determine sample sizes but our sample sizes are similar to those reported in previous publications.
Data exclusions	No data were excluded.
Replication	All experiments were performed with multiple replicates, and standard statistical methods were used to accept. Technical replicates were used for in vitro experiments where biological factors were not present, whereas biological replicates were used for the in vivo studies.
Randomization	Mice were assigned randomly to the experimental groups.
Blinding	The investigators were not blinded to allocation during experiments and outcome assessment since our data analyses are based on objectively measurable data.

Reporting for specific materials, systems and methods

We require information from authors about some types of materials, experimental systems and methods used in many studies. Here, indicate whether each material, system or method listed is relevant to your study. If you are not sure if a list item applies to your research, read the appropriate section before selecting a response.

Materials & experimental systems

n/a	Involved in the study
☐	☒ Antibodies
☐	☒ Eukaryotic cell lines
☒	☐ Palaeontology and archaeology
☐	☒ Animals and other organisms
☒	☐ Clinical data
☒	☐ Dual use research of concern

Methods

n/a	Involved in the study
☒	☐ ChIP-seq
☐	☒ Flow cytometry
☒	☐ MRI-based neuroimaging

Antibodies

Antibodies used

Anti-CD16/CD32 (93, 14016186, eBioscience), 1:20 dilution;
CD45 Rat anti-Mouse (APC-efluor780, Clone: 30 F11), 1:100 dilution;
CD3e Armenian Hamster anti-Mouse (PerCP-Cy5.5, Clone: 145 2C11, eBioscience), 1:100 dilution;
CD4 Rat anti-Mouse (PE-Cy7, Clone: GK1.5, eBioscience), 1:100 dilution;
Foxp3 Monoclonal Antibody (APC, Clone: FJK-16s, eBioscience), 1:50 dilution;
IL-4 Rat anti-Mouse (PE, Clone: 11B11, eBioscience), 1: 100 dilution;
IL-10 Rat anti-Mouse (FITC, Clone: JES5-16E3, eBioscience), 1: 100 dilution;
anti-mouse IFN-γ (BV421, Clone: XMG1.2, Biolegend), 1: 100 dilution;
T-bet Mouse anti-Human, Mouse (PE, Clone: 4B10, eBioscience), 1: 100 dilution;
GATA-3 Rat anti-Mouse (Alexa Fluor™ 488, Clone: TWAJ, eBioscience), 1: 100 dilution;
RORγt Mouse anti-Mouse (BV421, Clone: Q31-378, BD), 1:100 dilution;
CD11c Armenian Hamster Monoclonal Antibody (PE-Cy7, clone: N418, Biolegend), 1:250 dilution;
anti-mouse CX3CR1 (BV605, Clone: SA011F11, Biolegend), 1:100 dilution;
CD103 Rat anti-Mouse (PE,Clone: M290, BD), 1:100 dilution;
anti-mouse I-A/I-E (FITC, Clone: M5/114.15.2, Biolegend), 1:200 dilution;
F4/80 Rat anti-Mouse F4/80 (BV711, Clone: T45 2342, BD Biosciences), 1:250 dilution.

BV785-Anti-CD11c Armenian Hamster Monoclonal Antibody (Clone: N418, BioLegend), 1:250 dilution;
PerCP/Cy5.5-anti-mouse/human CD11b (Clone: M1/70, BioLegend), 1:100 dilution;
AF594-anti-mouse CD80 (Clone: B7-1), 1:100 dilution;
APC-anti-mouse CD86 (Clone: B7-2, BioLegend), 1:100 dilution;
BV421-CD45 Rat Monoclonal Antibody (Clone: 30-F11, BioLegend), 100 dilution;
Pacific Blue-CD19 Rat Monoclonal Antibody (Clone: 6D5, BioLegend), 100 dilution;
BV510-anti-mouse I-A/I-E antibody (Clone: M5/114.15.2, BioLegend), 1:200 dilution;
BV711-Anti-Ly6C Rat Monoclonal Antibody (Clone: HK1.4, BioLegend), 100 dilution;
FITC-anti-mouse/human CD11b (Clone: M1/70, BioLegend), 1:100 dilution;
PE-Anti-CD64 Mouse Monoclonal Antibody (Clone: X54-5/7.1, BioLegend), 1:100 dilution;
PE/Cy7-anti-mouse Ly6G (Clone: 1A8, BioLegend), 1:100 dilution;
AF647-Siglec-F Rat anti-mouse (Clone: E50 2440, BD), 1:100 dilution;
AF700-anti-CD3 Rat Monoclonal Antibody (Clone: 17A2, BioLegend), 1:100 dilution.

Cd28 Hamster anti-Mouse (NA/LE, Unlabeled, Clone: 37.51, BD), 1:200 dilution;
Cd3ε Hamster anti Mouse (NA/LE, Unlabeled, Clone: 145 2C11, BD),1:200 dilution;
anti-IL-4 antibody (clone 11B11, BioXCell), used in vivo without dilution;
anti-IFN-γ (clone XMG1.2; BioXcell), used in vivo without dilution;
anti-IL-10 (clone JES5-2A5; BioXcell), used in vivo without dilution;
Rat IgG1 isotype control (clone HRPN; BioXcell), used in vivo without dilution.

TotalSeq™-C0301 anti-mouse Hashtag 1 antibody (BioLegend), 1:50 dilution;
TotalSeq™-C0302 anti-mouse Hashtag 2 antibody (BioLegend), 1:50 dilution;
TotalSeq™-C0303 anti-mouse Hashtag 3 antibody (BioLegend), 1:50 dilution.

Validation

Antibody validation was provided by manufacture's website (cell images) and/or data is provided in the paper.

Eukaryotic cell lines

Policy information about cell lines and Sex and Gender in Research

Cell line source(s)

The Foxp3(GFP) CD4 T cell line was obtained from spleen in Foxp3(GFP) reporter mice. The CD4 T cell line was obtained from spleen in the wide-type C57BL/6 mice. The OT-II CD4 T cell line was obtained from spleen in OT-II mice.

Authentication

CD4 T cells isolated from spleen in wide-type or transgenic mice, while these mice were authenticated by the provider (The Jackson Laboratory). No further authentication of the isolated CD4 T cells was performed.

Mycoplasma contamination

All cell lines tested negative for mycoplasma contamination.

Commonly misidentified lines
(See ICLAC register)

No commonly misidenified cell lines were used.

Animals and other research organisms

Policy information about studies involving animals; ARRIVE guidelines recommended for reporting animal research, and Sex and Gender in Research

Laboratory animals	For the in vivo studies, 5-6 weeks-old female BALB/c mice (Jackson Laboratory, 18–20 g), 5-6 weeks-old female C3H/HeJ mice (Jackson Laboratory, 18–20 g), 5-7 weeks-old female C57BL/6 mice (Jackson Laboratory, 18–20 g) were used. OT-II mice and Foxp3(GFP) reporter transgenic mice (7 weeks-old female, 15–20 g) were obtained from the Jackson Laboratory. Mice were housed in 12-hour light–dark cycle, at 72 F, and about 30% humidity.
Wild animals	The study did not involve wild animals.
Reporting on sex	Female mice were used based on the previously published results.
Field-collected samples	The study did not involve samples collected from the field.
Ethics oversight	All work performed on animals was in accordance with, and approved by, the Institutional Animal Care & Use Committee (IACUC) at University of Michigan, Ann Arbor.

Note that full information on the approval of the study protocol must also be provided in the manuscript.

Flow Cytometry

Plots

Confirm that:

☒ The axis labels state the marker and fluorochrome used (e.g. CD4-FITC).

☒ The axis scales are clearly visible. Include numbers along axes only for bottom left plot of group (a 'group' is an analysis of identical markers).

☒ All plots are contour plots with outliers or pseudocolor plots.

☒ A numerical value for number of cells or percentage (with statistics) is provided.

Methodology

Sample preparation	The sample preparation is described in Methods.
Instrument	Ze5 cell analyzer (BD Biosciences), Cytek Aurora analyzer (Cytek Biosciences).
Software	FlowJo (v.10.5) (Tree Star) were used for data analysis.
Cell population abundance	Data on the abundance of relevant cell populations are provided in the paper.
Gating strategy	Cells were gated first by morphology to exclude cell debris, doublets were then gated out by FSC-H/FSC-W, SSC-H/SSC-W, followed by exclusion of dead cells by gating on dye-negative cells.

☒ Tick this box to confirm that a figure exemplifying the gating strategy is provided in the Supplementary Information.